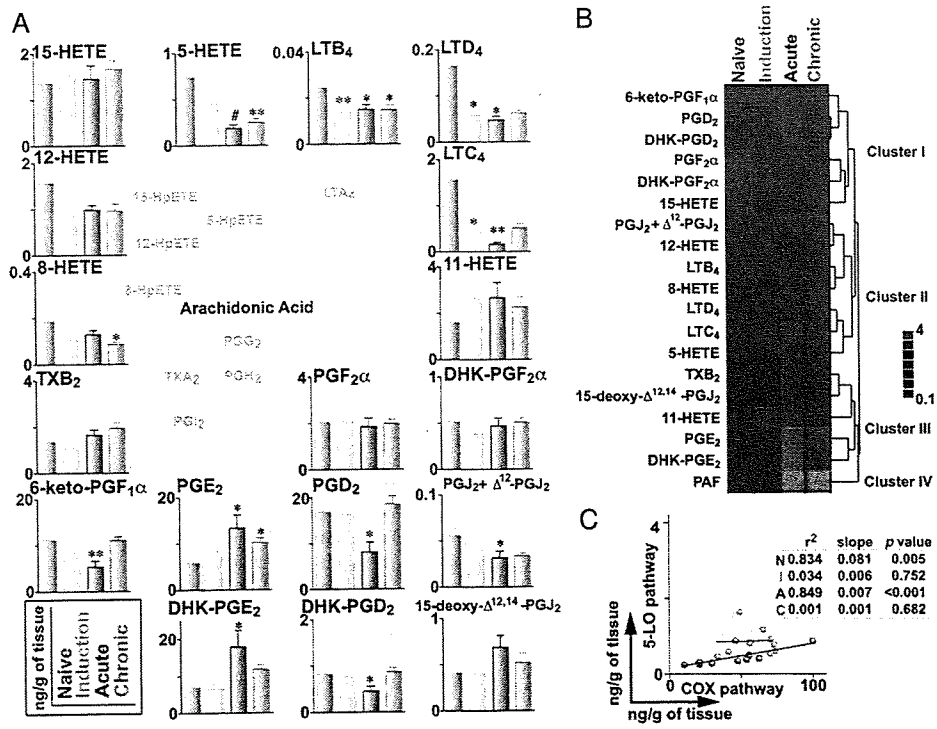

Fig. 2. AA cascade-targeted metabolomics analysis. (*A*) Eicosanoid levels in the SCs of naive mice and EAE mice in the induction, acute, and chronic phases (n = 8–10 animals) were determined. Data represent means ± SEM. #, $P < 0.001$, **, $P < 0.01$, *, $P < 0.05$ compared with naive mice using the Kruskal-Wallis test with Dunn's post-hoc test. (*B*) The means of eicosanoid levels were normalized with those of naive mice for each eicosanoid. Then, a cluster analysis was performed by the Ward method. The normalized eicosanoid levels were divided into seven levels according to the indicated color scale. (*C*) Correlations of COX/5-LO in naive mice (light blue) and EAE mice in the induction (pink), acute (red), and chronic (orange) phases are shown (n = 8–10 animals). Each data point represents the results from a single animal. Data were analyzed statistically by Pearson's correlation.

mPGES-1 Is Expressed in Human MS Lesions. To investigate whether the mPGES-1 is a therapeutic target in MS patients, we examined autopsy brain tissues obtained from MS patients (Fig. 4). In accordance with murine EAE (Fig. 3*A*), immunohistochemistry on MS lesions revealed the overt expression of mPGES-1 protein (Fig. 4 *A*, *B*, *D*, and *E*) in $CD68^-$ macrophages (Fig. 4 *G*–*Q*). Immunoreactivity of mPGES-1 was not detected with antigen-absorbed Ab (Fig. 4 *C* and *F*). These data suggest that not only murine EAE, but also human MS pathology seems to be influenced by the mPGES-1-PGE_2 axis of the AA cascade.

Discussion

In the present study, we provided a comprehensive overview of the AA cascade dynamics in EAE lesions and determined the roles of mPGES-1 and PGE_2 in EAE. By the AA cascade-targeted lipidomics approach, we found that the PGE_2 pathway is favored and the PGD_2, PGI_2, and 5-LO pathways are attenuated. Correlation analysis imply that the AA producing enzyme $cPLA_2\alpha$ possibly passes more AA to the COX than the 5-LO pathway in EAE, because the sequential actions of eicosanoid-synthesizing enzymes are regulated spatially and temporally in the cells, the so-called functional coupling (16–18). Likewise, PGH_2, a common precursor of PGs, appears to be selectively consumed by the PGE_2 pathway rather than the PGI_2 and PGD_2 pathways, thereby producing PGE_2 in the SCs of EAE mice.

The symptoms of EAE in $COX\text{-}2^{-/-}$ mice were comparable to those of wild-type controls and administration of indomethacin, a nonselective COX inhibitor, prevented development of the disease (14). We found that COX-2 expression was substantially up-regulated in the SCs of EAE mice from the induction phase (Fig. 1*B*). The absolute number of microglia/macrophages increased before the onset and throughout the disease course (23), and COX-2 is generally induced by the inflammatory mediators in these cells (24), implying that the up-regulation of COX-2 depended on these cells. In human MS, Rose et al. reported the COX-2 expression in microglia/macrophages of MS lesions (25). We demonstrated here that COX-1 mRNA expression is up-regulated in the SCs of EAE mice (Fig. 1*B*) and is correlated with clinical symptoms (Fig. S2). Deininger and Schluesener showed the constitutive expression of COX-1 in the microglia/macrophages of rat brain and an elevation of its expression levels in the cells with the progression of EAE (26). Further studies are needed to disclose the functions of COX-1 and COX-2 in EAE pathology.

Among the eicosanoids examined, only the PGE_2 level was significantly elevated in the SCs of EAE mice (Fig. 2). This up-regulation seems to depended on the mPGES-1 expressed in the microglia/macrophages of EAE lesions, because the PGE_2 production was almost completely suppressed in $mPGES\text{-}1^{-/-}$ mice (Fig. 3*B*). The expression of EP1, EP2, and EP4 was altered depending on the disease severity (Fig. 1*B* and Fig. S2). Therefore, these EPs are candidates for the downstream effectors of PGE_2. Indeed, the exogenous and endogenous PGE_2 activates EP2 and EP4 on antigen presenting cells to stimulate expression of IL-23 and IL-6, resulting in a shift toward T_H17 responses (27–30). PGE_2 synergized with IL-23 in expanding human T_H17 cell (31) and directly promoted differentiation of human and murine T_H17 cells through

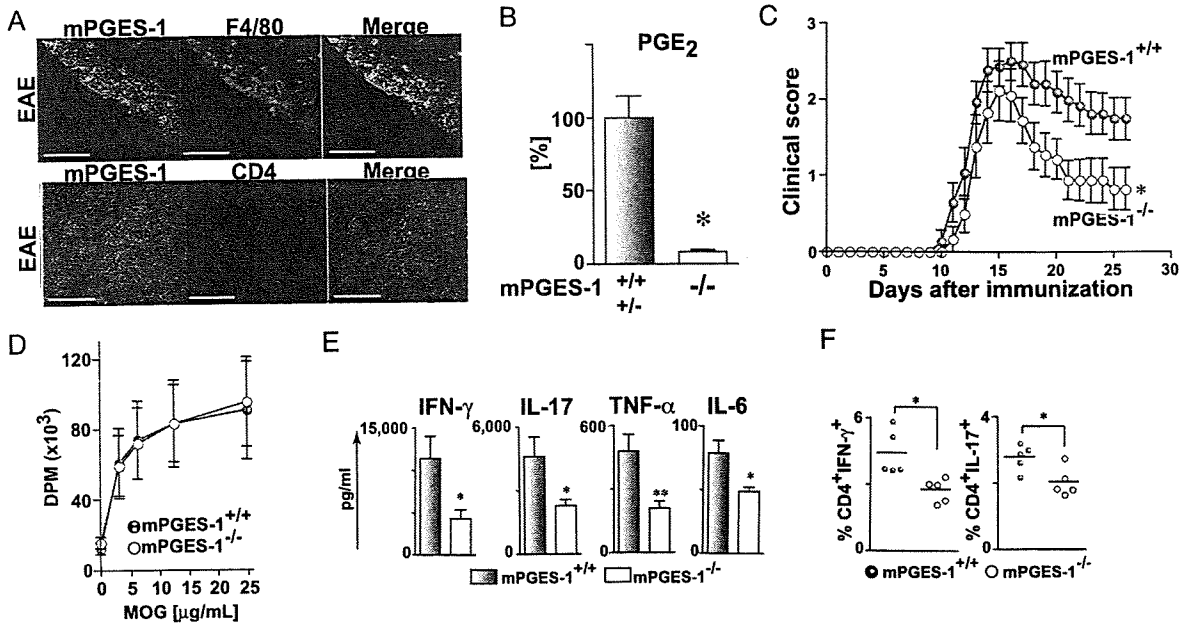

Fig. 3. Suppression of EAE pathology and T_H1/T_H17 responses in the absence of mPGES-1. (*A*) SCs of EAE mice in the acute phase were stained with anti-mPGES-1 (green), F4/80 (red), and CD4 (red) Abs. (Scale bar, 50 μm.) These pictures are representative of two different experiments. (*B*) PGE_2 levels were measured in the SCs of mPGES-$1^{+/-}$, $^{-/-}$ and mPGES-$1^{-/-}$ mice on day 26 (n = 13 and 7 animals, respectively). *, $P < 0.05$ versus mPGES-$1^{+/+}$, $^{+/-}$ mice by Mann–Whitney U test. Data represent means ± SEM. (*C*) mPGES-$1^{+/+}$ (filled circles) and mPGES-$1^{-/-}$ (open circles) mice were immunized with the MOG_{35-55} peptide and clinical scores were assessed daily for 26 days. Data represent means ± SEM from two independent experiments with a total of 14 and 9 animals for mPGES-$1^{+/+}$ and mPGES-$1^{-/-}$ mice, respectively. *, $P <$ 0.0001 versus mPGES-$1^{+/+}$ mice determined by two-way repeated measures ANOVA. (*D*) LN cells from EAE-induced mPGES-$1^{+/+}$ and mPGES-$1^{-/-}$ mice on day 11 were stimulated in vitro with various concentrations of MOG_{35-55} peptide, and the proliferative responses were measured (n = 5 animals). Data represent means ± SEM. (*E*) Supernatants of LN cell cultures were used to measure the concentrations of IFN-γ, IL-17, TNF-α, and IL-6 (n = 5 animals). Data represent means ± SEM. *, $P < 0.05$, **, $P < 0.01$ versus mPGES-$1^{-/-}$ mice by two-tailed Student's t test. (*F*) Two days after activation, cells were restimulated with PMA/ionomycin and subjected to intracellular cytokine staining for IFN-γ and IL-17 (n = 5 animals). Each data point represents the results from a single animal and the horizontal bars designate the mean values of individual groups. *, $P < 0.05$, by two-tailed Student's t test.

EP2/EP4 signaling (32). In addition, Yao et al. (30) recently reported that PGE_2 acting on EP4 on T cells amplifies IL-23-mediated T_H17 expansion in vitro and an EP4-selective antagonist suppressed the EAE pathology. In the case of T_H1 immune responses, differentiation of T_H1 cells from naive T cells in vitro was facilitated by EP1 (33), EP2, or EP4 agonists (30). T cells appear to encounter the autoantigens mainly in the peripheral lymphoid organs in the induction phase, and then in inflammatory foci of CNS in the acute and chronic phases. The levels of PGE_2 in the spleen were unchanged during the disease course (Fig. S4), whereas those in the SCs were drastically elevated in wild-type mice (Fig. 2). Furthermore, the EAE pathology of mPGES-$1^{-/-}$ mice was attenuated in the chronic phase. These results imply that EP4-expressing T cells are affected by PGE_2 in the CNS rather than in peripheral lymphoid organs. We showed that the mPGES-1 deficiency abrogated the T_H1 and T_H17 cytokine production in EAE (Fig. 3 *E* and *F*), suggesting that PGE_2 produced by microglia/macrophages in inflammatory foci may aggravate EAE by promoting the differentiation of T_H1 and the expansion of T_H17 cells through these EPs (Fig. 5).

We found that the PGIS expression was essentially diminished in EAE-induced C57BL/6 mice, resulting in a significant decrease of 6-keto-$PGF_{1\alpha}$ levels in the acute phase of EAE (Fig. 2). Because PGI_2 enhances endothelial barrier function (34), PGI_2 seems to protect mice from EAE by suppressing the inflammatory cell infiltration. Several reports showed that loss of mPGES-1 results in the rediversion of a substrate PGH_2 to other prostanoids, like PGI_2, which may affect the physiological and pathophysiological conditions of mPGES-$1^{-/-}$ mice (35–37). Therefore, it is possible that the amelioration of EAE in mPGES-$1^{-/-}$ mice is due to the up-regulation of PGI_2 levels (Fig. S6). On the other hand, the collagen-induced arthritis was aggravated by the PGI_2-IP axis (38), raising another possibility that the PGI_2 is an exacerbating factor in T_H1 and T_H17 immune responses and EAE pathology. The roles of PGI_2 in EAE pathology remain controversial, and further studies are needed.

Reduction in PGD_2 levels in the acute phase and its recovery in the chronic phase could be explained by the expression changes of L-PGDS (Figs. 1*B* and 2). One of the features of EAE/MS is demyelination, which coincides with oligodendrocyte cell death. L-PGDS is thought to be an anti-apoptotic molecule that protects oligodendrocytes, because the oligodendrocyte apoptosis was enhanced in the brain of L-PGDS-deficient twitcher mice (39). In human MS, L-PGDS expression was increased especially in the remyelinated lesions (40). Thus, the decrease and the subsequent recovery of L-PGDS may be associated with the demyelination and remyelination in EAE/MS, respectively. Another PGD synthase, H-PGDS, showed the pattern opposite to L-PGDS expression (Fig. 1*B*). Although H-PGDS is highly expressed in hematopoietic cells and microglia/macrophages (41), PGD_2 levels were not elevated in the SCs of EAE mice in the acute phase. Because these cells also express mPGES-1, COX-1/2 seem to prefer to functionally couple with mPGES-1 rather than H-PGDS in the cells of EAE lesions.

Contrary to the up-regulation of 5-LO/FLAP transcripts (Fig. 1*B*), we demonstrated here the significant suppression of 5-LO metabolites during EAE pathology (Fig. 2). The discrepancy be-

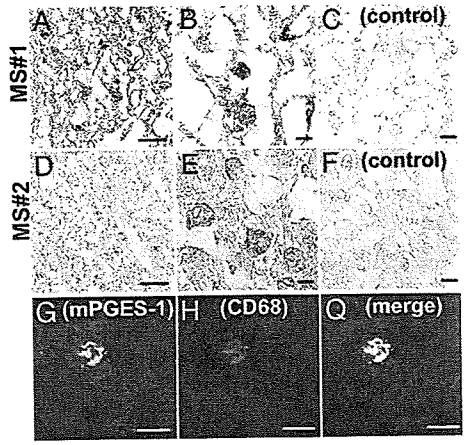

Fig. 4. mPGES-1 expression in infiltrated macrophages of MS lesions. Brain tissues of MS patients' autopsied materials displaying periventricular demyelinating lesions were stained with anti-mPGES-1. (Scale bar, 50 μm *A*, *B*, *D*, and *E*.) The high magnification images of *A* and *D* are shown in *B* and *E*, respectively. (Scale bar, 10 μm.) The antigen-peptide blocks the signals of anti-mPGES-1 Ab staining. (Scale bar, 10 μm *C* and *F*.) Both MS #1 (subacute stage, *A–C*) and MS #2 (acute stage, *D–F*) showed extensive infiltration of macrophages characterized by foamy appearance. The mPGES-1 is colocalized with CD68-immunoreactive macrophage in the MS lesions. (Scale bar, 10 μm *G–Q*.)

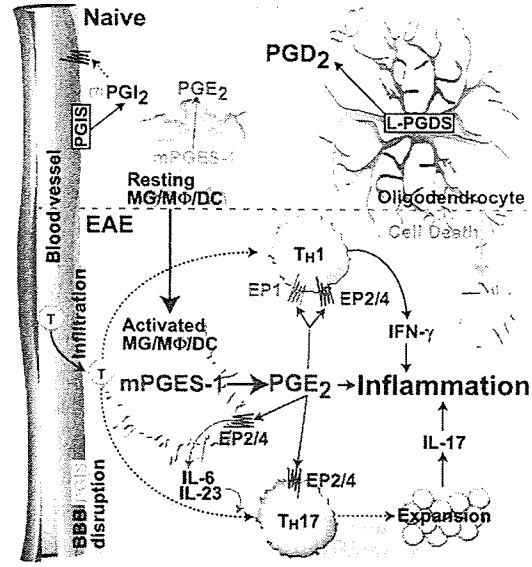

Fig. 5. Conceptual model for the role of AA cascade in EAE pathology. PGE_2 is produced by mPGES-1 in activated microglia (MG), infiltrating macrophages (MΦ) and dendritic cells (DC), and then activates these cells in an autocrine/paracrine manner through EP2/EP4. T cells differentiate into T_H17 cells by stimulation with IL-6 and IL-23 secreted from activated MG/MΦ/DC. T_H1 differentiation and expansion of T_H17 cells are accelerated by the direct effects of PGE_2 on EP1 and EP2/EP4.

tween transcripts and metabolites is explained by posttranscriptional/translational (such as phosphorylation) regulation of enzymes (42–44) and/or functional coupling with $cPLA_2\alpha$. Furthermore, COX enzymes were up-regulated in the SC around the same time (Fig. 1*B*), which results in the reduction of the substrate availability for 5-LO. Emerson and LeVine reported that 5-$LO^{-/-}$ mice developed more severe EAE than control wild-type mice (15), suggesting a possibility of increased PGE_2 production in the SCs of 5-$LO^{-/-}$ mice. Meanwhile, the report raises another possibility that lipid mediators downstream of 5-LO may play protective roles in EAE pathology. Because Gladue et al. (45) showed that a BLT1 antagonist protects mice from EAE, LTB_4 is not such a candidate for the protective lipid mediators. 5-LO generates not only LTs but also lipoxins and resolvins (46, 47), which are anti-inflammatory/proresolving lipid mediators derived from AA and eicosapentaenoic acid, respectively, although we did not measure these lipid mediators in the current study. 12/15-LO deficiency conferred more severe EAE pathology (15), possibly because 12/15-LO also mediates lipoxin production. Resolvin E1 reduces dendritic cell migration and IL-12 production, suggesting a protective role in EAE pathology (48).

As a therapeutic strategy, blocking the hub of the AA cascade, like COX-1/2, seems to be highly effective in preventing EAE pathology. Although treatment of indomethacin actually ameliorates EAE, all mice died of gastrointestinal ulcers and bleeding (14), a well-known side effect of NSAIDs (49). In 2004, rofecoxib, a selective COX-2 inhibitor, was withdrawn because of an increased cardiovascular risk in patients taking the drug for >18 months (50, 51). A possible reason why NSAIDs are currently only used for treatment of flu-like symptoms associated with IFN therapy for MS is that inhibition of COX-1/2 may put the patients at high risk for adverse effects. Therefore, it seems that targeting AA cascade downstream of COX-1/2 is highly effective in treating MS without side effects. As discussed above, components of AA cascade contribute to EAE pathology via intricate mechanisms (Fig. 5), while our AA cascade-targeted lipidomics approach and knockout study identified the mPGES-1-PGE_2-EPs axis as the critical pathway of AA cascade in EAE pathology. Given the function of EPs in T_H1 and T_H17 immune responses (27–29, 38) and our findings of mPGES-1 expression in MS lesions (Fig. 4), inhibition of mPGES-1 has a much better chance of blocking individual EPs. Although mPGES-1 inhibitors which effectively suppress PGE_2 production in rodents (22) have not been published yet, MF63, a selective human mPGES-1 inhibitor, suppressed PGE_2 production, pyresis and inflammatory pain in knock-in mouse expressing human mPGES-1 (52). We believe that mPGES-1 inhibitors provide a significant treatment option for MS.

Materials and Methods

Mice. Female C57BL/6 mice were purchased from Charles River for lipidomics analysis. The mPGES-$1^{-/-}$ mice were generated as described in ref. 53. See *SI Materials and Methods* for more information.

Induction of EAE. Mice were s.c. immunized with MOG_{35-55} peptide. Pertussis toxin was i.p. injected. See *SI Materials and Methods* for more information.

Quantification of Eicosanoids and mRNA Levels in SCs. Eicosanoid levels were estimated simultaneously as described in refs. 13, 19, 54, and 55. See *SI Materials and Methods* for more information.

Ex Vivo Experiments. The details of recall responses to the MOG_{35-55} peptide antigen, ELISA, and flow cytometry are provided in *SI Materials and Methods*.

Immunohistochemistry. For murine EAE, SCs obtained from EAE-induced mice were stained with either anti-F4/80 (Serotec) or CD4 (BD Biosciences) Ab and mPGES-1 (Affinity BioReagents) Ab as primary Abs. For human MS, cerebral specimens were stained with rabbit anti-human mPGES-1 polyclonal Ab (Cayman) or mouse anti-human CD68 monoclonal Ab (DAKO, clone KP1) as a first Ab. See *SI Materials and Methods* for more information.

Statistical Analysis. As appropriate, data were analyzed statistically by means of a Student's *t* test, Mann–Whitney *U* test, Fisher's exact test, two-way repeated measures ANOVA, or Kruskal-Wallis test with Dunn's post-hoc test. Statistical,

clustering, and correlation analyses were performed using JMP6 (SAS Institute) or Prism 4 (GraphPad). P values <0.05 were considered to be statistically significant.

ACKNOWLEDGMENTS. We thank Drs. T. Yokomizo (Kyushu University), N. Uozumi, K. Masago, and K. Yanagida (University of Tokyo) for valuable suggestions and Drs. T. Iwaki and S. Suzuki (Kyushu University) for providing autopsied MS samples. This work was supported, in part, by Grants-in-Aid for Scientific Research from the Ministry of Education, Science, Culture, Sports, and Technology of Japan (T.S., S.I., Y. Kita, and J.-i.K.), Health and Labor Sciences Research Grants for the Comprehensive Research on Aging and Health (S.I.) and the Research on Allergic disease and Immunology (S.I.) from the Ministry of Health, Labor and Welfare of Japan, grants to the Respiratory Failure Research Group (S.I.) and the Research Committee of Neuroimmunological Diseases (J.-i.K.) from the Ministry of Health, Labor and Welfare of Japan, a grant from the Kato Memorial Trust for Nambyo Research (S.I.), and the Research Fellowships of Japanese Society for the Promotion of Science (Y. Kihara).

1. McFarland HF, Martin R (2007) Multiple sclerosis: A complicated picture of autoimmunity. *Nat Immunol* 8:913–919.
2. Bettelli E, Korn T, Oukka M, Kuchroo VK (2008) Induction and effector functions of T(H)17 cells. *Nature* 453:1051–1057.
3. Bettelli E, Oukka M, Kuchroo VK (2007) T(H)-17 cells in the circle of immunity and autoimmunity. *Nat Immunol* 8:345–350.
4. Kroenke MA, Carlson TJ, Andjelkovic AV, Segal BM (2008) IL-12- and IL-23-modulated T cells induce distinct types of EAE based on histology, CNS chemokine profile, and response to cytokine inhibition. *J Exp Med* 205:1535–1541.
5. Kanter JL, et al. (2006) Lipid microarrays identify key mediators of autoimmune brain inflammation. *Nat Med* 12:138–143.
6. Shimizu T (2009) Lipid mediators in health and disease: Enzymes and receptors as therapeutic targets for the regulation of immunity and inflammation. *Annu Rev Pharmacol Toxicol* 49:123–150.
7. Shimizu T, Ohto T, Kita Y (2006) Cytosolic phospholipase A2: Biochemical properties and physiological roles. *IUBMB Life* 58:328–333.
8. Funk CD (2001) Prostaglandins and leukotrienes: Advances in eicosanoid biology. *Science* 294:1871–1875.
9. Narumiya S, FitzGerald GA (2001) Genetic and pharmacological analysis of prostanoid receptor function. *J Clin Invest* 108:25–30.
10. Kalyvas A, David S (2004) Cytosolic phospholipase A2 plays a key role in the pathogenesis of multiple sclerosis-like disease. *Neuron* 41:323–335.
11. Marusic S, et al. (2005) Cytosolic phospholipase A2 alpha-deficient mice are resistant to experimental autoimmune encephalomyelitis. *J Exp Med* 202:841–851.
12. Marusic S, et al. (2008) Blockade of cytosolic phospholipase A(2)alpha prevents experimental autoimmune encephalomyelitis and diminishes development of Th1 and Th17 responses. *J Neuroimmunol* 204:29–37.
13. Kihara Y, et al. (2008) Platelet-activating factor production in the spinal cord of experimental allergic encephalomyelitis mice via the group IVA cytosolic phospholipase A2-Lyso-PAFAT axis. *J Immunol* 181:5008–5014.
14. Miyamoto K, et al. (2006) Selective COX-2 inhibitor celecoxib prevents experimental autoimmune encephalomyelitis through COX-2-independent pathway. *Brain* 129:1984–1992.
15. Emerson MR, LeVine SM (2004) Experimental allergic encephalomyelitis is exacerbated in mice deficient for 12/15-lipoxygenase or 5-lipoxygenase. *Brain Res* 1021:140–145.
16. Murakami M, Kambe T, Shimbara S, Kudo I (1999) Functional coupling between various phospholipase A2s and cyclooxygenases in immediate and delayed prostanoid biosynthetic pathways. *J Biol Chem* 274:3103–3115.
17. Murakami M, et al. (2000) Regulation of prostaglandin E2 biosynthesis by inducible membrane-associated prostaglandin E2 synthase that acts in concert with cyclooxygenase-2. *J Biol Chem* 275:32783–32792.
18. Ueno N, et al. (2001) Coupling between cyclooxygenase, terminal prostanoid synthase, and phospholipase A2. *J Biol Chem* 276:34918–34927.
19. Kihara Y, et al. (2005) Dual phase regulation of experimental allergic encephalomyelitis by platelet-activating factor. *J Exp Med* 202:853–863.
20. Hofstetter AO, et al. (2007) The induced prostaglandin E2 pathway is a key regulator of the respiratory response to infection and hypoxia in neonates. *Proc Natl Acad Sci USA* 104:9894–9899.
21. Ikeda-Matsuo Y, et al. (2006) Microsomal prostaglandin E synthase-1 is a critical factor of stroke-reperfusion injury. *Proc Natl Acad Sci USA* 103:11790–11795.
22. Samuelsson B, Morgenstern R, Jakobsson PJ (2007) Membrane prostaglandin E synthase-1: A novel therapeutic target. *Pharmacol Rev* 59:207–224.
23. Ponomarev ED, Shriver LP, Maresz K, Dittel BN (2005) Microglial cell activation and proliferation precedes the onset of CNS autoimmunity. *J Neurosci Res* 81:374–389.
24. Smith WL, DeWitt DL, Garavito RM (2000) Cyclooxygenases: Structural, cellular, and molecular biology. *Annu Rev Biochem* 69:145–182.
25. Rose JW, Hill KE, Watt HE, Carlson NG (2004) Inflammatory cell expression of cyclooxygenase-2 in the multiple sclerosis lesion. *J Neuroimmunol* 149:40–49.
26. Deininger MH, Schluesener HJ (1999) Cyclooxygenases-1 and -2 are differentially localized to microglia and endothelium in rat EAE and glioma. *J Neuroimmunol* 95:202–208.
27. Sheibanie AF, Khayrullina T, Safadi FF, Ganea D (2007) Prostaglandin E2 exacerbates collagen-induced arthritis in mice through the inflammatory interleukin-23/interleukin-17 axis. *Arthritis Rheum* 56:2608–2619.
28. Sheibanie AF, et al. (2004) Prostaglandin E2 induces IL-23 production in bone marrow-derived dendritic cells. *FASEB J* 18:1318–1320.
29. Sheibanie AF, et al. (2007) The proinflammatory effect of prostaglandin E2 in experimental inflammatory bowel disease is mediated through the IL-23–>IL-17 axis. *J Immunol* 178:8138–8147.
30. Yao C, et al. (2009) Prostaglandin E2-EP4 signaling promotes immune inflammation through TH1 cell differentiation and TH17 cell expansion. *Nat Med* 15:633–640.
31. Chizzolini C, et al. (2008) Prostaglandin E2 (PGE2) synergistically with interleukin-23 (IL-23) favors human Th17 expansion. *Blood* 112:3696–3703.
32. Boniface K, et al. (2009) Prostaglandin E2 regulates Th17 cell differentiation and function through cyclic AMP and EP2/EP4 receptor signaling. *J Exp Med* 206:535–548.
33. Nagamachi M, et al. (2007) Facilitation of Th1-mediated immune response by prostaglandin E receptor EP1. *J Exp Med* 204:2865–2874.
34. Fukuhara S, et al. (2005) Cyclic AMP potentiates vascular endothelial cadherin-mediated cell–cell contact to enhance endothelial barrier function through an Epac-Rap1 signaling pathway. *Mol Cell Biol* 25:136–146.
35. Boulet L, et al. (2004) Deletion of microsomal prostaglandin E2 (PGE2) synthase-1 reduces inducible and basal PGE2 production and alters the gastric prostanoid profile. *J Biol Chem* 279:23229–23237.
36. Trebino CE, et al. (2005) Redirection of eicosanoid metabolism in mPGES-1-deficient macrophages. *J Biol Chem* 280:16579–16585.
37. Wang M, et al. (2006) Deletion of microsomal prostaglandin E synthase-1 augments prostacyclin and retards atherogenesis. *Proc Natl Acad Sci USA* 103:14507–14512.
38. Honda T, Segi-Nishida E, Miyachi Y, Narumiya S (2006) Prostacyclin-IP signaling and prostaglandin E2-EP2/EP4 signaling both mediate joint inflammation in mouse collagen-induced arthritis. *J Exp Med* 203:325–335.
39. Taniike M, et al. (2002) Perineuronal oligodendrocytes protect against neuronal apoptosis through the production of lipocalin-type prostaglandin D synthase in a genetic demyelinating model. *J Neurosci* 22:4885–4896.
40. Kagitani-Shimono K, et al. (2006) Lipocalin-type prostaglandin D synthase (beta-trace) is upregulated in the alphaB-crystallin-positive oligodendrocytes and astrocytes in the chronic multiple sclerosis. *Neuropathol Appl Neurobiol* 32:64–73.
41. Kanaoka Y, Urade Y (2003) Hematopoietic prostaglandin D synthase. *Prostaglandins Leukot Essent Fatty Acids* 69:163–167.
42. Haeggstrom JZ (2004) Leukotriene A4 hydrolase/aminopeptidase, the gatekeeper of chemotactic leukotriene B4 biosynthesis. *J Biol Chem* 279:50639–50642.
43. Radmark O, Werz O, Steinhilber D, Samuelsson B (2007) 5-Lipoxygenase: Regulation of expression and enzyme activity. *Trends Biochem Sci* 32:332–341.
44. Welsch DJ, et al. (1994) Molecular cloning and expression of human leukotriene-C4 synthase. *Proc Natl Acad Sci USA* 91:9745–9749.
45. Gladue RP, et al. (1996) Inhibition of leukotriene B4-receptor interaction suppresses eosinophil infiltration and disease pathology in a murine model of experimental allergic encephalomyelitis. *J Exp Med* 183:1893–1898.
46. Serhan CN, Chiang N, Van Dyke TE (2008) Resolving inflammation: Dual anti-inflammatory and pro-resolution lipid mediators. *Nat Rev Immunol* 8:349–361.
47. Serhan CN, Savill J (2005) Resolution of inflammation: The beginning programs the end. *Nat Immunol* 6:1191–1197.
48. Arita M, et al. (2005) Stereochemical assignment, antiinflammatory properties, and receptor for the omega-3 lipid mediator resolvin E1. *J Exp Med* 201:713–722.
49. Wolfe MM, Lichtenstein DR, Singh G (1999) Gastrointestinal toxicity of nonsteroidal anti-inflammatory drugs. *N Engl J Med* 340:1888–1899.
50. James MJ, Cook-Johnson RJ, Cleland LG (2007) Selective COX-2 inhibitors, eicosanoid synthesis and clinical outcomes: A case study of system failure. *Lipids* 42:779–785.
51. Juni P, et al. (2004) Risk of cardiovascular events and rofecoxib: Cumulative meta-analysis. *Lancet* 364:2021–2029.
52. Xu D, et al. (2008) MF63 [2-(6-chloro-1H-phenanthro[9,10-d]imidazol-2-yl)-isophthalonitrile], a selective microsomal prostaglandin E synthase-1 inhibitor, relieves pyresis and pain in preclinical models of inflammation. *J Pharmacol Exp Ther* 326:754–763.
53. Uematsu S, Matsumoto M, Takeda K, Akira S (2002) Lipopolysaccharide-dependent prostaglandin E(2) production is regulated by the glutathione-dependent prostaglandin E(2) synthase gene induced by the Toll-like receptor 4/MyD88/NF-IL6 pathway. *J Immunol* 168:5811–5816.
54. Kita Y, et al. (2005) Pathway-oriented profiling of lipid mediators in macrophages. *Biochem Biophys Res Commun* 330:898–906.
55. Kita Y, Takahashi T, Uozumi N, Shimizu T (2005) A multiplex quantitation method for eicosanoids and platelet-activating factor using column-switching reversed-phase liquid chromatography-tandem mass spectrometry. *Anal Biochem* 342:134–143.

Research Paper

Multiple Sclerosis

Multiple Sclerosis
15(12) 1411–1421

DOI: 10.1177/1352458509348961
msj.sagepub.com
SAGE

Association of anti-*Helicobacter pylori* neutrophil-activating protein antibody response with anti-aquaporin-4 autoimmunity in Japanese patients with multiple sclerosis and neuromyelitis optica

Wei Li*, Motozumi Minohara*, Hua Piao, Takuya Matsushita, Katsuhisa Masaki, Takeshi Matsuoka, Noriko Isobe, Jen Jen Su, Yasumasa Ohyagi and Jun-ichi Kira

Abstract

There are two distinct subtypes of multiple sclerosis (MS) in Asians: opticospinal (OSMS) and conventional (CMS). OSMS has similar features to neuromyelitis optica (NMO) and half of OSMS patients have the NMO-Immunoglobulin G (IgG)/anti-aquaporin-4 (AQP4) antibody. We reported that *Helicobacter pylori* (*H. pylori*) infection was significantly less common in CMS patients than controls. To reveal the immune responses to the *H. pylori* neutrophil-activating protein (HP-NAP) in Japanese MS patients, according to anti-AQP4 antibody status, sera from 162 MS patients, 37 patients with other inflammatory neurological diseases (OIND), and 85 healthy subjects were assayed for anti-*H. pylori* antibodies, anti-HP-NAP antibodies, and myeloperoxidase (MPO) by enzyme immunoassays. *H. pylori* seropositivity rates were significantly higher in anti-AQP4 antibody-positive MS/NMO (AQP4 + /MS) patients (19/27, 70.4%) than anti-AQP4 antibody-negative CMS (AQP4 − /CMS) patients (22/83, 26.5%). Among *H. pylori*-infected individuals, the anti-HP-NAP antibody was significantly more common in AQP4 + /MS and AQP4 − /OSMS patients than healthy subjects (36.8%, 34.6% versus 2.8%). Among the AQP4 + /MS patients, a significant positive correlation between anti-HP-NAP antibody levels and the final Kurtzke's Expanded Disability Status Scale scores was found, and MPO levels were higher in anti-HP-NAP antibody-positive patients than anti-HP-NAP antibody-negative ones. Therefore, HP-NAP may be associated with the pathology of anti-AQP4 antibody-related neural damage in MS/NMO patients.

Keywords

multiple sclerosis, aquaporin-4, *Helicobacter pylori*, neutrophil-activating protein, opticospinal, neuromyelitis optica, Japanese

Date received: 18th February 2009; accepted: 12th August 2009

Introduction

Multiple sclerosis (MS) is a demyelinating disease of the central nervous system (CNS). In Asians, MS is rare; however, when it appears, selective but severe involvement of the optic nerves and spinal cord is characteristic. This form, termed opticospinal MS (OSMS), is observed in 15–40% of Japanese MS patients, with the remainder having features that are similar to those of MS in Caucasians (conventional MS (CMS)).[1] Recent studies, including Japan's fourth nationwide survey of MS, disclosed a sharp rise in the ratio of CMS patients to OSMS patients in the Japanese population, especially among those born after Japan's period of rapid economic growth, together with an increase in the overall prevalence of MS.[2,3] Because the environment during childhood has a critical effect on susceptibility to MS, environmental

Department of Neurology, Neurological Institute, Graduate School of Medical Sciences, Kyushu University, Fukuoka 812-8582, Japan.

*These authors contributed equally to this work.

Corresponding author:
Jun-ichi Kira, Department of Neurology, Neurological Institute, Graduate School of Medical Sciences, Kyushu University, Fukuoka 812-8582, Japan.
Email: kira@neuro.med.kyushu-u.ac.jp

changes accompanying Japan's Westernization may have altered the incidence and phenotypes of MS in the Japanese.

Helicobacter pylori (*H. pylori*) are gram-negative microaerophilic bacteria that reside in the stomachs of more than 50% of the entire human population.[4] Because *H. pylori* infection occurs early in childhood, via water-borne transmission, and persists throughout life,[5] the infection rate is dependent on the water source.[6] Improvements in sanitation in Japan have reduced the prevalence of *H. pylori* in people born after the 1950s.[7] We disclosed that *H. pylori* seropositivity was significantly lower in patients with CMS compared with healthy controls, and that in CMS patients, *H. pylori* seropositivity showed a significant inverse association with mean Expanded Disability Status Scale (EDSS) score and fulfillment of the Barkhof criteria for brain magnetic resonance imaging (MRI) lesions.[8] A similar low prevalence of *H. pylori* infection was also reported in MS patients in Western populations.[9] *H. pylori* infection is thus suggested to be a protective factor against CMS.

On the other hand, OSMS has similar features to the relapsing form of neuromyelitis optica (NMO) in Westerners.[1] Both selectively affect the optic nerves and spinal cord, in which axons as well as myelin are involved. The nosological position of NMO has long been a matter of debate. However, the discovery of a specific Immunoglobulin G (IgG) against NMO, designated NMO-IgG,[10] recognizing aquaporin-4 (AQP4),[11] suggests that NMO is a distinct disease entity with a fundamentally different etiology from MS. Because the anti-AQP4 antibody has been reported to be present in 50–60% of OSMS patients with longitudinally extensive spinal cord lesions (LESCLs),[12,13] OSMS has been suggested to be the same entity as NMO. However, the mechanisms underlying the development of LESCLs in Asians appear to be heterogeneous; namely, there are anti-AQP4 antibody-related and -unrelated mechanisms.[12] However, the mechanism underlying anti-AQP4 antibody production and its role in lesion formation still remains ill defined.

Many studies published in the past decade indicate a relationship between *H. pylori* infection and extragastric inflammatory disorders.[14–17] Persistent *H. pylori* infection could be a chronic inflammatory stimulus to hosts. *H. pylori* neutrophil-activating protein (HP-NAP) is one of the major proinflammatory proteins responsible for the pathology of *H. pylori*-related gastric inflammatory conditions.[18] HP-NAP is capable of crossing epithelial monolayers and induces migration and the activation of neutrophils.[18] In both OSMS and NMO, abundant neutrophil infiltration occurs in the acute lesions.[19,20] Furthermore, we also found activation of peripheral blood neutrophils and systemic inflammation in OSMS patients, especially those with the anti-AQP4 antibody.[21] These observations prompted us to study the prevalence of *H. pylori* infection and the immune response to HP-NAP in Japanese patients with MS, according to the anti-AQP4 antibody status.

Methods

Patients

We conducted a retrospective analysis of 162 consecutive patients (41 men and 121 women) with MS, diagnosed according to the criteria of McDonald et al.[22] at the Department of Neurology, Kyushu University Hospital, between 1997 and 2007. The age at examination was 39.7 years (median; range: 14–73 years) and the age at disease onset was 30.8 years (range: 9–70 years). There were no obvious symptoms of gastropathy, such as gastric and duodenal ulcers, at the time of blood sampling. Patients were classified according to anti-AQP4 antibody status, as determined by the immunofluorescence method described below, and clinical phenotypes were divided into three subtypes: anti-AQP4 antibody-positive MS/NMO (AQP4 + /MS), anti-AQP4 antibody-negative OSMS (AQP4 – /OSMS), and anti-AQP4 antibody-negative CMS (AQP4 – /CMS), as described previously.[12,23,24] Briefly, 27 patients were positive for the anti-AQP4 antibody while 135 patients were negative for the antibody. Among the AQP4 + /MS patients, 81.5% (22/27) had an OSMS phenotype while 18.5% (5/27) had a CMS phenotype, and 70.4% (19/27) fulfilled the 2006 Wingerchuk's criteria for NMO;[25] therefore, we describe this patient group as AQP4 + /MS patients in subsequent sections. Among anti-AQP4 antibody-negative patients, 38.5% (52/135) of patients whose clinically estimated main lesions were confined to the optic nerves and spinal cord were classified as AQP4 – /OSMS patients. These patients had no clinical evidence of disease in either the cerebrum or cerebellum, but minor brainstem signs, such as transient double vision and nystagmus, were acceptable.[23] The remaining 61.5% (83/135) of patients had multiple involvement of the CNS, including the cerebrum, cerebellum, and brainstem, and were classified as AQP4 – /CMS patients.[23] In addition, 37 patients with other inflammatory neurological diseases (OIND) (27 patients with HTLV-I-associated myelopathy and 10 patients with encephalitis; nine men and 28 women), and 85 healthy subjects (21 men and 64 women) were enrolled as control subjects. The age at sampling was 53.0 years (range: 15–77 years) in OIND patients and 42.0 years (range: 21–64 years) in healthy controls. The ages at onset and the time of blood sampling were significantly higher in

OIND patients than in AQP4 – /OSMS and CMS patients (age at onset: $p = 0.0018$ and $p < 0.001$, respectively, and age at time of blood sampling: $p = 0.019$ and $p < 0.001$, respectively). The disability status of MS patients was scored by one of the authors (TM) using Kurtzke's EDSS.[26] Severe optic neuritis was defined as grade 5 or more than 5 on Kurtzke's Visual Functional Scale (FS) [26]. The progression index was determined by dividing the EDSS scores by disease duration (years).[27] Acute transverse myelitis (ATM) was defined according to Fukazawa et al.[28] The study procedures were approved by the ethics committee of the Graduate School of Medical Sciences, Kyushu University.

*Anti-*H. pylori *antibody assay*

As described in a previous report,[8] serum *H. pylori* antibodies were measured using the SMITEST ELISA helicobacter (Chemicon, Australia) according to the manufacturer's instructions. In brief, serum specimens, along with positive and negative controls, were diluted 1 : 201 with a dilution buffer (10 µl of serum in 2000 µl of the dilution buffer) and 100 µl of each diluted sample was added to a well on the ELISA plate before being incubated for 15 minutes at room temperature; then, the plate was washed three times with the washing buffer provided. One hundred microliters of freshly prepared horseradish peroxidase-IgG conjugate reagent was added to each well, and the plate was incubated for 15 minutes at room temperature. After repeat washings, 100 µl of substrate reagent was added to each well and the plate was incubated in the dark for 15 minutes at room temperature. Stopping solution (100 µl) was added to each well to terminate the enzymatic reaction. The absorbance was read within 30 minutes with a 450 nm filter. The antibody concentration of *H. pylori* was read from the calibration curve of standards. The cut-off value of the assay was 50 U/ml, and any reading greater than this cut-off value was considered positive for *H. pylori* infection.

*Detection of anti-*Chlamydia pneumoniae *IgG, anti-varicella-zoster virus IgG and anti-Epstein-Barr virus nuclear antigen IgG antibodies*

Anti-*Chlamydia pneumoniae* (*C. pneumoniae*) IgG, anti-varicella-zoster virus (VZV) IgG, and anti-Epstein-Barr nuclear antigen (EBNA) IgG levels were measured using commercial ELISA kits according to the manufacturer's instructions (VIRCELL, Spain). The antibody index was determined by dividing the optical density (O.D.) values for target samples by the O.D. values for negative control samples and expressed as a percentage.

HP-NAP preparation

For expression, the *nap*A reading frame was amplified by polymerase chain reaction (PCR) from the *H. pylori* strain with the primers ThioNAP-kpn-01 (5'-GGCGGGTACCGATGAAAACATTTG -3') and ThioNAP-pst1-02 (5'- CGCTGCAGTTAAGCCAAA TGAGCT -3'), and cloned into the *pThioHis A* expression vector included in the *E. coli* His-Patch ThioFusion™ Expression System (Invitrogen, Carlsbad, CA). The clones were confirmed by restriction digestion and sequencing, and then *pThioHis-NAP* was obtained. Thereafter, the plasmid was transformed into the *E. coli Top 10* strain (Invitrogen). *E. coli* were grown overnight at 37°C in 10 ml of Luria-Bertani (LB) containing ampicillin (100 µg/ml), subcultured into 1 L of LB/ampicillin, and grown for 3 hours at 37°C. *E. coli* was induced for 3 hours with isopropyl-thio-β-D-galactoside (IPTG) at a final concentration of 1 mM, and the cells were collected by centrifugation and disrupted by sonication. After centrifugation, the supernatants were run through a ProBond column (Invitrogen) and HP-NAP was extracted by elution buffer (25 mM Tris-HCl, 0.5 M NaCl, 250 mM imidazole) and dialysed with 25 mM Tris-HCl buffer (pH 8.0) in 1 mM EDTA. Then, to remove the endotoxins of *E. coli*, polymyxin B agarose gel filtration column chromatography (Sigma-Aldrich, St. Louis, MO) was performed and the concentrations of endotoxins were measured using a Limulus amebocyte lysate assay kit (BioWhittaker, Walkersville, Maryland).

Enzyme-linked immunosorbent assay for HP-NAP

We measured the levels of serum IgG against HP-NAP in 163 MS patients, 37 OIND patients, and 85 healthy controls by ELISA. A cut-off value for positivity was set as the mean +4 SD in healthy controls whose *H. pylori* infection was negative based on the results of preliminary experiments. HP-NAP (2 µg/ml) was applied to 96-well plates (ICN Biomedicals, Aurora, Ohio) in the presence of 50 µl of bicarbonate coating the buffer (15 mM Na_2CO_3, 35 mM $NaHCO_3$ [pH 9.6]) at 4°C overnight. After being washed three times in 0.01% Tween 20 in Phosphate Buffered Saline (PBS) (PBS-T20), the plates were blocked with 20% blocking buffer (Nacalai Tesque, Japan) for 45 minutes at room temperature. Then, the serum samples were diluted 1 : 100 in PBS-T20 and 50 µl of the diluted samples was added to each well and incubated at room temperature for 1 hour. After repeat washes, 50 µl aliquots of 1 : 2000-diluted horseradish peroxidase-conjugated mouse anti-human IgG antibody (Southern Biotechnology Associates, Birmingham, AL) were added to the plates, which were incubated at room

temperature for 1 hour. The plates were washed again, 100 μl of SIGMA FAST o-phenylenediamine dihydrochloride (Sigma-Aldrich) was added to each well, and the plates were incubated in the dark for 15 minutes at room temperature. The reaction was stopped by 4 M sulfuric acid and the results were read within 30 minutes with a 450 nm filter in the spectrophotometer. The newly developed ELISA for HP-NAP had intra- and inter-assay CVs of 8.0% and 5.9%, respectively.

Assay measuring inhibition of anti-AQP4 antibody by HP-NAP

Assays measuring the inhibition of the anti-AQP4 antibody by HP-NAP were performed in a liquid phase using serum samples obtained from four anti-HP-NAP seropositive patients (three AQP4 + /MS patients and one AQP4 – /OSMS patient). The sera were preincubated at 37°C for 1 hour in PBS containing 100 μg/ml of HP-NAP or bovine serum albumin as a control. After preincubation, aliquots of the mixtures were transferred to HP-NAP-coated plates and assessed as described above for ELISA; the remaining mixtures were used for measurement of the anti-AQP4 antibody by an immunofluorescence method using GFP-AQP4 fusion protein-transfected HEK293 cells, as previously described.[12]

Myeloperoxidase sandwich enzyme immunoassay

The myeloperoxidase (MPO) level was measured by a sandwich enzyme immunoassay according to the manufacturer's standard protocol (Immundiagnostik AG, Benshein, Germany), as described in a previous report.[21] Serum samples were thawed from −80°C to room temperature and assayed in duplicate in 96-well polystyrene microtiter plates coated with a capture antibody. A peroxidase-conjugated polyclonal anti-human MPO antibody was used in the assays, and tetramethylbenzidine was used as a peroxidase substrate. The lower detection limit was 1.6 ng/ml. All antibody assays were performed by one of the authors (WL) without knowledge of the specimens.

Magnetic resonance imaging

All magnetic resonance (MR) studies were performed with a 1.5-T Magnetom Vision and Symphony (Siemens Medical Systems, Erlangen, Germany) MRI scanner, as described previously.[12] Brain and spinal cord MR images were evaluated independently by two of the authors (JS and T Matsuoka) who were naive to the diagnoses. Brain MRI lesions were evaluated according to the Barkhof criteria.[29] Spinal cord lesions extending over three or more vertebral lengths were considered to be LESCLs.

Statistical analysis

Statistical analyses of ages at time of onset and blood sampling, disease duration, relapse rate, progression index, EDSS score, and antibody index were initially performed using the Kruskal–Wallis H test. When statistical significance was found, the Mann–Whitney U test was used to determine the statistical significance of differences among subgroups. Uncorrelated p-values were corrected by multiplying by the number of comparisons (Bonferroni-Dunn's correction). Differences in ratios among subgroups were tested for significance by Fisher's exact test. The correlation of anti-HP-NAP antibody titers with various clinical parameters was analysed by Spearman's rank correlation test. In all assays, significance was defined as $P < 0.05$.

Results

Demographic features of the patients according to the anti-AQP4 antibody status

The demographic features of the patients are summarized in Table 1. The proportion of females was significantly greater among AQP4 + /MS patients than among AQP4 – /CMS patients ($P = 0.01$). The ages at onset and time of blood sampling were significantly higher in AQP4 + /MS patients than in AQP4 – /CMS patients ($P = 0.044$ and $P = 0.038$, respectively). The disease durations at the time of blood sampling and final follow-up, and the EDSS at final follow-up, did not differ significantly among AQP4 + /MS, AQP4 – /OSMS and AQP4 – /CMS patients. The frequency of brain lesions fulfilling the Barkhof criteria was significantly higher in AQP4 – /CMS patients than in AQP4 + /MS and AQP4 – /OSMS patients ($P < 0.001$), while the frequency of LESCLs was higher in AQP4 + /MS patients than in AQP4 – /OSMS and AQP4 – /CMS patients ($P < 0.001$). The relapse rate was significantly greater in AQP4 + /MS patients than in AQP4 – /CMS patients ($P = 0.0078$), but there was no significant difference in progression index among the three groups. Interferon (IFN)-beta treatment was more commonly performed in AQP4 – /CMS patients than in AQP4 + /MS and AQP4 – /OSMS patients (44.3% versus 14.8% and 20.4%, $P = 0.0177$, and $P = 0.0177$, respectively), but there was no significant difference among the three groups in terms of the chronic administration of low dosages of corticosteroids (prednisolone ≤20 mg/day).

Frequency of H. pylori seropositivity

The frequency of *H. pylori* seropositivity did not differ significantly between MS patients and healthy controls (67/162, 41.4% versus 36/85, 42.4%) (Figure 1(a)).

Table 1. Demographic features of the subjects

	Total MS ($n = 162$)	AQP4 + /MS ($n = 27$)	AQP4 – /OSMS ($n = 52$)	AQP4 – /CMS ($n = 83$)	OIND ($n = 37$)	HC ($n = 85$)
Male : Female	41 : 121 (1 : 3.0)	1 : 26[b]	11 : 41 (1 : 3.7)	29 : 54 (1 : 1.9)[b]	9 : 28 (1 : 3.1)	21 : 64 (1 : 3.0)
Age at onset (years)[a]	30.8 (9–70)	37.2 (15–65)[b]	32.9 (9–65)[c]	28.0 (10–70)[b,d]	50.0 (14–71)[c,d]	NA
Age at blood sampling (years)[a]	39.7 (14–73)	46.7 (27–68)[b]	44.5 (17–67)[c]	36.9 (14–73)[b,d,e]	53.0 (15–77)[c,d,f]	42.0 (21–64)[e,f]
Disease duration at blood sampling (months)[a]	66.7 (1–508)	57.0 (4–369)	65.8 (3–370)	71.0 (1–508)	51.0 (1–432)	NA
Disease duration at final follow-up (months)[a]	105.0 (5–523)	111.0 (37–461)	115.8 (6–391)	91.9 (5–523)	NA	NA
EDSS scores at final follow up[a]	3.5 (0–9.5)	5.0 (0–9.0)	3.0 (0–9.5)	3.5 (0–9.5)	NA	NA
Fulfillment of Barkhof criteria (%)	47.3	33.3[b]	18.8[c]	71.2[b,c]	NA	NA
Severe optic neuritis (≥FS 5) (%)	45.0	69.2[b]	58.0[c]	28.0[b,c]	NA	NA
ATM (%)	34.6	53.8[b]	58.1[c]	9.8[b,c]	NA	NA
LESCL (%)	42.9	77.8[b,c]	47.1[b]	27.6[c]	NA	NA
Relapse rate[a]	0.6 (0–2.7)	0.9 (0.2–2.7)[b]	0.6 (0.1–1.9)	0.5 (0–2.4)[b]	NA	NA
Progression index[a]	0.3 (0–8.5)	0.4 (0–1.5)	0.3 (0–4.6)	0.3 (0–8.5)	NA	NA
C. pneumoniae antibody seropositivity (%)	69.2	79.2	68.9	65.6	61.6	68.9
C. pneumoniae antibody index[a]	12.8 (0.4–19.6)	13.8 (2–17.7)	12.6 (0.6–16.9)	12.6 (0.4–19.6)	12.2 (0.9–16.2)	13.7 (0.8–18.0)
VZV antibody seropositivity (%)	98.5	95.8	100	98.4	97.4	100
VZV antibody index[a]	23.7 (6.1–30.9)	24.7 (7.6–29.9)	24.1 (16–30.9)	23.1 (6.1–29.9)	23.9 (10.9–27.2)	24.3 (13.4–28.7)
EBNA antibody seropositivity (%)	90.7	87.5	91.1	91.8	82.1	91.8
EBNA antibody index[a]	27.4 (0.3–36.5)	27.4 (2.5–36.5)	26.0 (0.3–35.0)	28.3 (0.4–36.5)	26.6 (1.3–35.9)	26.6 (1.3–35.9)
Low-dose corticosteroids (%)(≤20 mg)	9.0	14.8	10.2	6.3	NA	NA
IFN beta (%)	31.6	14.8[b]	20.4[c]	44.3[b,c]	NA	NA

[a]Median (range); [b,c,d,e,f] Statistically significant difference between the linked values ($P^{corr} < 0.05$).

AQP4, aquaporin-4; AQP4+, anti-AQP4 antibody-positive; AQP4–, anti-AQP4 antibody-negative; ATM, acute transverse myelitis; CMS, conventional form of multiple sclerosis; *C. pneumonia*, *Chlamydia pneumoniae*; EBNA, Epstein-Barr nuclear antigen; EDSS, Expanded Disability Status Scale of Kurtzke; FS, Kurtzke's Visual Functional Scale; HC, healthy controls; IFN, interferon; LESCL, longitudinally extensive spinal cord lesion; NA, not applicable; OIND, other inflammatory neurological diseases; OSMS, opticospinal form of multiple sclerosis; VZV, varicella-zoster virus.

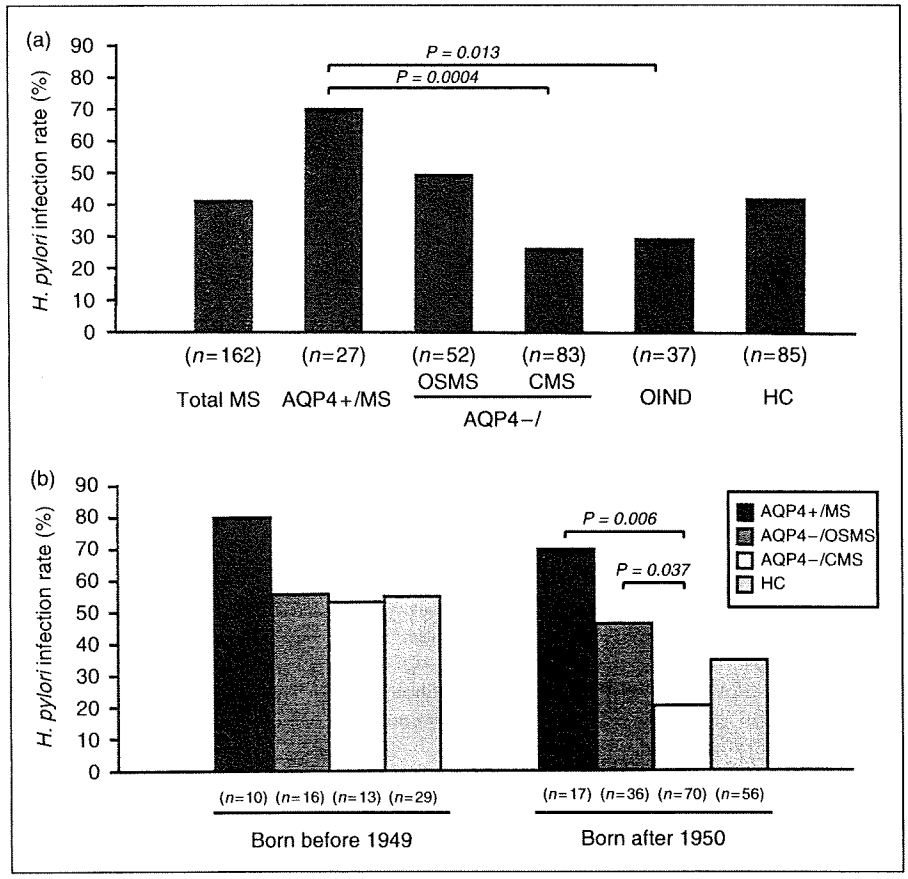

Figure 1. Frequency of *H. pylori* seropositivity in MS patients and controls. (a) The frequency of *H. pylori* seropositivity is shown according to the anti-AQP4 antibody status and clinical phenotype. Note that the *H. pylori* seropositivity rate is significantly higher in AQP4 + /MS patients than in AQP4 − /CMS patients. It is also significantly higher in AQP4 + /MS patients than in OIND patients. (b) Frequency of *H. pylori* seropositivity according to year of birth. Among patients born after 1950, the *H. pylori* seropositivity rate is significantly higher in AQP4 + /MS patients and AQP4 − /OSMS patients than in AQP4 − /CMS patients. AQP4, aquaporin-4; AQP4 − /CMS, anti-AQP4 antibody-negative conventional form of multiple sclerosis; AQP4 + /MS, anti-AQP4 antibody-positive multiple sclerosis; AQP4 − /OSMS, anti-AQP4 antibody-positive opticospinal form of multiple sclerosis; HC, healthy controls; *H. pylori*, *Helicobacter pylori*; OIND, other inflammatory neurological diseases.

However, when analysed separately based on the anti-AQP4 antibody status and clinical phenotype, *H. pylori* seropositivity was significantly higher in AQP4 + /MS patients (19/27, 70.4%; $P = 0.0004$) than AQP4 − /CMS patients (22/83, 26.5%). In addition, *H. pylori* seropositivity was significantly higher in AQP4 + /MS patients than in OIND patients (11/37, 27.7%; $P = 0.013$). Furthermore, when analysed separately by year of birth, in patients born after 1950, the *H. pylori* seropositivity rate was significantly greater in AQP4 + /MS patients (11/17, 64.7%; $P = 0.006$) and AQP4 − /OSMS patients (17/36, 47.2%; $P = 0.037$) than in AQP4 − /CMS patients (15/70, 21.4%). In patients born before 1949, the *H. pylori* seropositivity rate did not differ significantly among the subgroups and healthy controls, although it was still higher in AQP4 + /MS patients than in the other groups (Figure 1(b)). By contrast, seropositivity rates and antibody indices for *C. pneumonia*, VZV, and EBNA did not differ among the subgroups and controls (Table 1).

Frequency of anti-HP-NAP antibody positivity rate

Among subjects with the anti-*H. pylori* antibody, the frequency of antibodies against HP-NAP was significantly higher in AQP4 + /MS patients (7/19, 36.8%) and AQP4 − /OSMS patients (9/26, 34.6%) than in healthy controls (1/36, 2.8%; $P = 0.016$, and $P = 0.008$, respectively) (Figure 2). However, anti-HP-NAP antibody levels (absorbance at 450 nm, shown in Figure 2) in AQP4 + /MS patients were not significantly correlated with anti-AQP4 antibody titers ($P > 0.05$). To determine if there was any cross reactivity between the anti-HP-NAP antibody and the

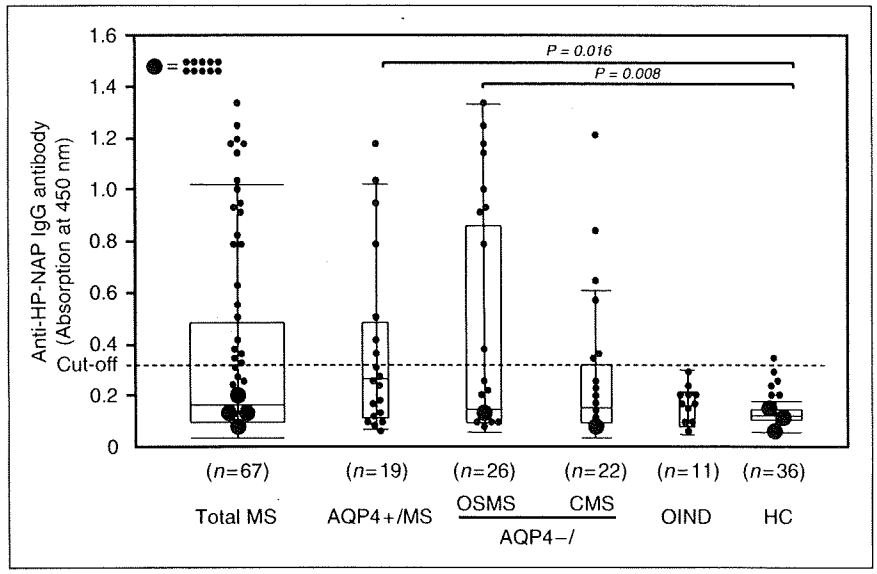

Figure 2. Anti-HP-NAP antibody levels in *H. pylori*-infected individuals. Among anti-*H. pylori* antibody-positive subjects, the frequency of the anti-HP-NAP antibody is significantly higher in AQP4 + /MS patients and AQP4 − /OSMS patients than in healthy controls. The cut-off value is set at the mean absorbance of the HC group +4S D. AQP4, aquaporin-4; AQP4 − /CMS, anti-AQP4 antibody-negative conventional form of multiple sclerosis; AQP4 + /MS, anti-AQP4 antibody-positive multiple sclerosis; AQP4 − /OSMS, anti-AQP4 antibody-positive opticospinal form of multiple sclerosis; HC, healthy controls; *H. pylori*, *Helicobacter pylori*; NAP, neutrophil-activating protein; OIND, other inflammatory neurological diseases.

anti-AQP4 antibody, four anti-HP-NAP antibody-positive serum samples were preabsorbed with 100 μg/ml of recombinant HP-NAP. This treatment completely abrogated the reactivity to HP-NAP in all four cases, while it did not affect anti-AQP4 antibody reactivity in any, including three anti-AQP4 antibody-positive cases.

Correlation between anti-HP-NAP antibody and clinical outcome

Anti-HP-NAP antibody levels were positively correlated with the final EDSS scores in all MS patients ($R = 0.248$, $P = 0.0022$). Among the subgroups, only AQP4 + /MS patients showed a significant positive correlation between anti-HP-NAP antibody levels and the final EDSS scores ($R = 0.405$, $P = 0.0299$), while no significant association between these parameters was observed in either AQP4 − /OSMS or AQP4 − /CMS patients (Figure 3(a)). Furthermore, in all MS patients, anti-HP-NAP antibody-positive patients had significantly greater EDSS scores than anti-HP-NAP antibody-negative patients (6.0 [range: 0–9.5] versus 3.5 [range: 0–9.5], respectively; $P = 0.0304$). Only in the AQP4 + /MS patient group did anti-HP-NAP antibody-positive subjects demonstrate significantly higher EDSS scores than anti-HP-NAP antibody-negative ones (6.0 [range: 5.0–9.0] versus 3.3 [range: 0–7.0], respectively; $P = 0.0312$), but no such difference based on anti-HP-NAP antibody status was found in either AQP4 − /OSMS or AQP4 − /CMS patients (Figure 3(b)). Among anti-*H. pylori* antibody-positive subjects, anti-HP-NAP antibody seropositivity had no significant correlation with the frequency of severe optic neuritis (≥FS 5.0), ATM, relapse rate, progression index, or abnormal MRI findings.

Relationship between myeloperoxidase level and anti-HP-NAP antibody status

We then compared MPO levels between anti-HP-NAP antibody-positive and -negative patients among the three subgroups of MS patients. Among AQP4 + /MS patients, MPO levels were significantly higher in anti-HP-NAP antibody-positive patients than anti-HP-NAP antibody-negative ones in the remission phase (170.6 ng/ml [range: 103–1970] versus 119.9 ng/ml, [range: 16–486], respectively; $P = 0.036$). A similar trend was also found in the relapse phase among AQP4 + /MS patients, but the difference between anti-HP-NAP antibody-positive and -negative subjects did not reach statistical significance owing to the small sample size (218.0 ng/ml [range: 81–1629] versus 145.7 ng/ml [range: 62–311], respectively; $P > 0.1$). By contrast, among both AQP4 − /OSMS and AQP4 − /CMS patients, there were no significant differences in MPO levels between anti-HP-NAP antibody-positive and -negative patients (Figure 4).

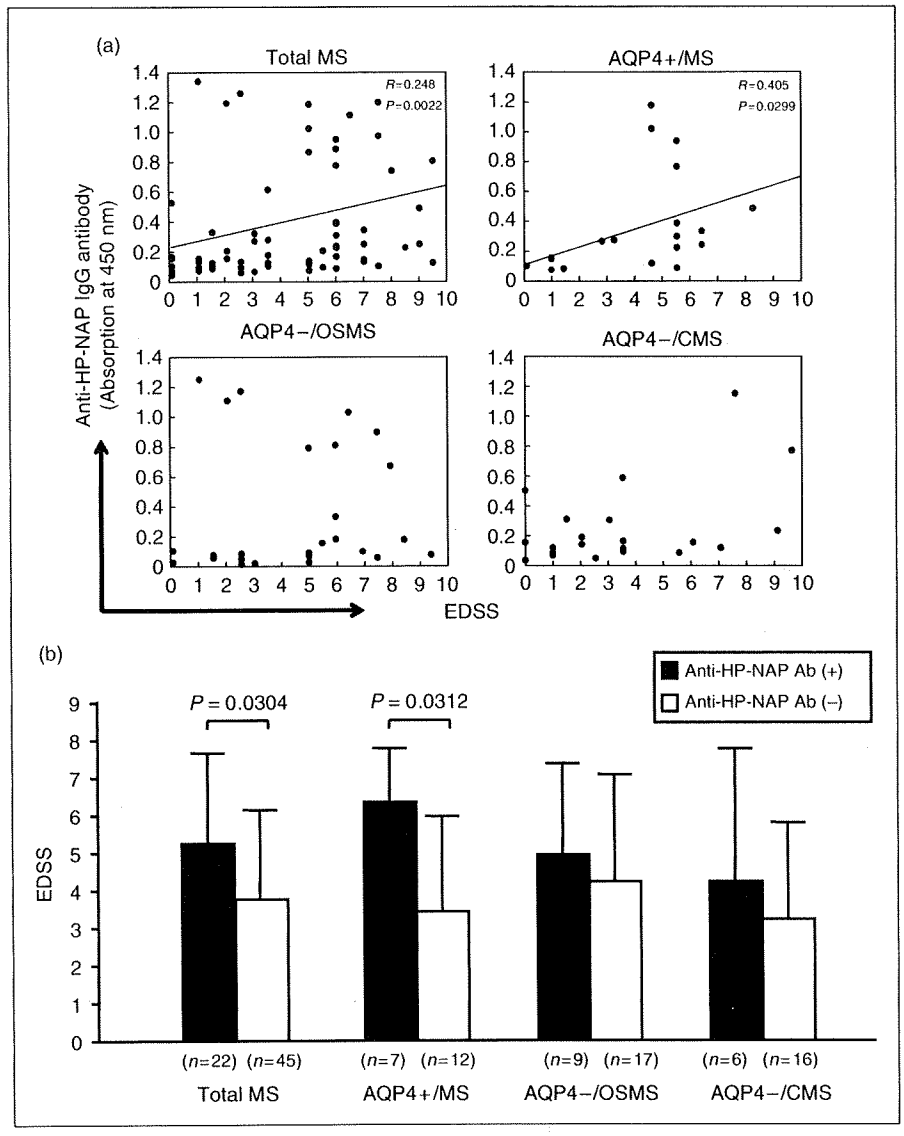

Figure 3. Relationship between the anti-HP-NAP antibody and the EDSS score. (a) Relationship between anti-HP-NAP antibody levels and final EDSS scores. In all MS patients and AQP4 + /MS patients, statistically significant positive correlations are seen between anti-HP-NAP antibody levels and final EDSS scores. (b) EDSS scores according to anti-HP-NAP antibody status. Among all MS patients and the AQP4 + /MS patient group, anti-HP-NAP antibody-positive patients show significantly higher EDSS scores than anti-HP-NAP antibody-negative ones. Ab, antibody; AQP4, aquaporin-4; AQP4 − /CMS, anti-AQP4 antibody-negative conventional form of multiple sclerosis; AQP4 + /MS, anti-AQP4 antibody-positive multiple sclerosis; AQP4 − /OSMS, anti-AQP4 antibody-positive opticospinal form of multiple sclerosis; EDSS, Expanded Disability Status Scale of Kurtzke; *H. pylori*, *Helicobacter pylori*; NAP, neutrophil-activating protein.

Discussion

The main new findings in the present study are as follows. (1) In *H. pylori*-infected individuals, the anti-HP-NAP antibody was significantly more common in AQP4 + /MS patients and AQP4 − /OSMS patients than controls. (2) Among the MS subgroups, only AQP4 + /MS patients showed a significant correlation between anti-HP-NAP antibody levels and final EDSS scores, and only among AQP4 + /MS patients did anti-HP-NAP antibody-positive subjects demonstrate significantly higher EDSS scores than anti-HP-NAP antibody-negative ones. (3) In AQP4 + /MS patients, MPO levels were significantly higher in anti-HP-NAP antibody-positive patients than in anti-HP-NAP antibody-negative ones in the remission phase, while a similar trend was also observed in the relapse phase.

Among anti-AQP4 antibody-negative MS patients, AQP4 − /CMS patients had a significantly lower frequency of *H. pylori* infection than AQP4 − /OSMS

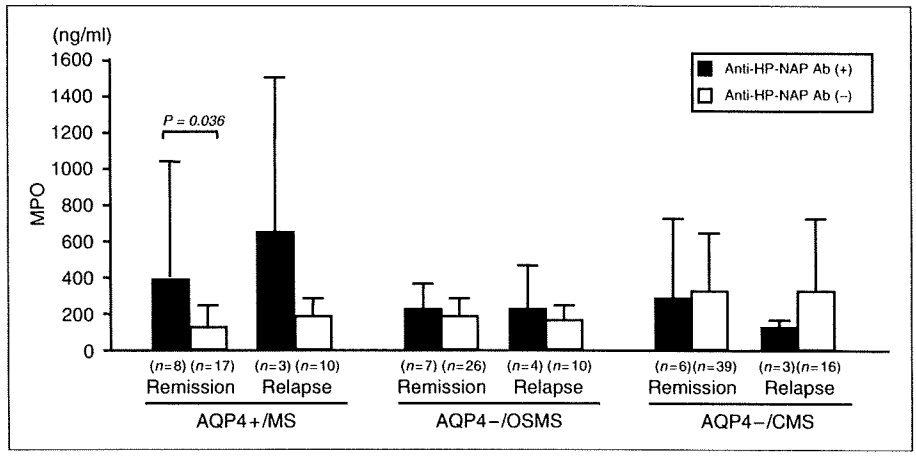

Figure 4. Relationship between MPO levels and anti-HP-NAP antibody seropositivity. Note that in the AQP4 + /MS patient group, MPO levels are significantly higher in anti-HP-NAP antibody-positive patients than in anti-HP-NAP antibody-negative patients in the remission phase; a similar trend is also seen in the relapse phase. No such difference based on anti-HP-NAP antibody status is seen in either AQP4 – /OSMS or AQP4 – /CMS patients. Ab, antibody; AQP4, aquaporin-4; AQP4 – /CMS, anti-AQP4 antibody-negative conventional form of multiple sclerosis; AQP4 + /MS, anti-AQP4 antibody-positive multiple sclerosis; AQP4 – /OSMS, anti-AQP4 antibody-positive opticospinal form of multiple sclerosis; HP, *Helicobacter pylori*; MPO, myeloperoxidase; NAP, neutrophil-activating protein.

patients, which is in accordance with the results of our previous report.[8] In addition, in the present study, we demonstrated that AQP4 + /MS patients had even higher frequencies of *H. pylori* infection than AQP4 – /CMS and AQP4 – /OSMS patients, especially in those born after 1950 when Japan's period of rapid economic growth began. *H. pylori* infection is supposed to occur mainly before the age of two years,[5] primarily because the parietal cells secreting gastric acids, which hamper the survival of *H. pylori*, are not mature in infancy.[4] Once acquired, the bacterium persistently colonizes the human stomach for years and decades;[4] thus, the difference in the *H. pylori* seropositivity rate indicates a distinction in the childhood infectious environment. Therefore, the sanitary environment during childhood is distinct between OSMS and CMS patients, and between AQP4 + /MS and AQP4 – /CMS patients: a clean environment is associated with CMS without the anti-AQP4 antibody, while an infectious one is associated with OSMS, and especially with MS/NMO with the anti-AQP4 antibody. Because an association between socioeconomic status and the risk of MS has been suggested to exist in Western countries,[30] the relationships among childhood socioeconomic status, *H. pylori* infection, and the occurrence of MS subtypes, in the Japanese, will be worth studying in the future.

The frequency of *H. pylori* infection has been reported to be increased in patients with some chronic inflammatory diseases, such as rheumatoid arthritis,[17] thyroiditis,[14] and autoimmune thrombocytopenic purpura.[15,16] Although the mechanism underlying this increase is ill defined, either a chronic inflammatory stimulus induced by *H. pylori* or cross mimicry between bacterial and host antigens is assumed to be responsible. We recently reported that, in AQP4 + /OSMS (NMO) patients, a high frequency of elevated C-reactive protein (CRP) and hypercomplementemia exist in the relapse phase,[31] indicating the presence of systemic inflammation. In OSMS (NMO) patients, spinal cord lesions are heavily infiltrated with MPO-positive granulocytes,[19,20] and neutrophilic pleocytosis in the cerebrospinal fluid (CSF) is occasionally seen in these conditions.[1] We also reported that the IL-17/IL-8 system, which induces neutrophil activation and migration, is upregulated in the CSF of OSMS patients,[20] irrespective of the presence or absence of the anti-AQP4 antibody,[32] and that the serum MPO level was significantly increased in OSMS patients and was positively correlated with EDSS scores.[21] Thus, neutrophils and a systemic inflammatory reaction appear to constitute a part of the potent effector arm of OSMS/NMO. Interestingly, anti-HP-NAP antibody levels were significantly positively correlated with both final EDSS scores and MPO levels in AQP4 + /MS patients in the present study. In individuals with the anti-HP-NAP antibody, HP-NAP is supposed to be absorbed in hosts and presented to the host immune system. HP-NAP acts not only directly on neutrophils and monocytes by promoting their recruitment and activation,[33,34] but also induces mast cells to release proinflammatory molecules that are able to activate neutrophils and monocytes.[33,34] Furthermore, *H. pylori* has been shown to strongly activate Th17 cells via induction of IL-23,[35,36] resulting in neutrophil

mobilization and activation. It is therefore conceivable that *H. pylori* infection and the proinflammatory protein HP-NAP contribute to the pathology of anti-AQP4 antibody-related neural damage, by acting as a systemic inflammatory stimulus targeting neutrophils.

Because HP-NAP itself did not bind to the anti-AQP4 antibody, molecular mimicry between HP-NAP and AQP4 is unlikely. However, bacteria harbor their own water channel proteins with some sequence homology to human AQP4.[37] Thus, molecular mimicry between human AQP4 and bacterial AQP is worth exploring for a possible source of cross-reactive antigens for the anti-AQP4 antibody.

In conclusion, *H. pylori* infection seems to be one of the risk factors for the development of AQP4 + /MS. Because of the retrospective nature of the present study, the occurrence of gastropathy might have been overlooked. Therefore, the results of the present study indicate that careful observation of the development of gastropathy and the eradication of *H. pylori* may be warranted in MS/NMO patients with *H. pylori* infection and the anti-AQP4 antibody as a possible adjunctive therapy.

Acknowledgment

This work was supported in part by a Neuroimmunological Disease Research Committee grant from the Ministry of Health, Labor and Welfare, Japan.

References

1. Kira J. Multiple sclerosis in the Japanese population. *Lancet Neurol* 2003; 2: 117–127.
2. Kira J, Yamasaki K, Horiuchi I, Ohyagi Y, Taniwaki T, Kawano Y. Changes in the clinical phenotypes of multiple sclerosis during the past 50 years in Japan. *J Neurol Sci* 1999; 166: 53–57.
3. Osoegawa M, Kira J, Fukazawa K, et al. Temporal changes and geographical differences in multiple sclerosis phenotypes in Japanese: nationwide survey results over 30 years. *Mult Scler* 2009; 15: 159–173.
4. Blaser MJ. *Helicobacter pylori*: microbiology of a 'slow' bacterial infection. *Trends Microbiol* 1993; 1: 255–259.
5. Graham DY. *Helicobacter pylori*: its epidemiology and its role in duodenal ulcer disease. *J Gastroenterol Hepatol* 1991; 6: 105–113.
6. Horiuchi T, Ohkusa T, Watanabe M, Kobayashi D, Miwa H, Eishi Y. *Helicobacter pylori* DNA in drinking water in Japan. *Microbiol Immunol* 2001; 45: 515–519.
7. Asaka M, Kimura T, Kudo M, et al. Relationship of *Helicobacter pylori* to serum pepsinogens in an asymptomatic Japanese population. *Gastroenterology* 1992; 102: 760–766.
8. Li W, Minohara M, Sun JJ, et al. *Helicobacter pylori* is a potential protective factor against conventional multiple sclerosis in the Japanese population. *J Neuroimmunol* 2007; 184: 227–231.
9. Wender M. Prevalence of *Helicobacter pylori* infection among patients with multiple sclerosis. *Neurol Neurochir Pol* 2003; 37: 45–48. (in Polish).
10. Lennon VA, Wingerchuk DM, Kryzer TJ, et al. A serum autoantibody marker of neuromyelitis optica: distinction from multiple sclerosis. *Lancet* 2004; 364: 2106–2112.
11. Lennon VA, Kryzer TJ, Pittock SJ, et al. IgG marker of optic-spinal multiple sclerosis binds to the aquaporin-4 water channel. *J Exp Med* 2005; 202: 473–477.
12. Matsuoka T, Matsushita T, Kawano Y, et al. Heterogeneity of aquaporin-4 autoimmunity and spinal cord lesions in multiple sclerosis in Japanese. *Brain* 2007; 130: 1206–1223.
13. Tanaka K, Tani T, Tanaka M, et al. Anti-aquaporin 4 antibody in selected Japanese multiple sclerosis patients with long spinal cord lesions. *Mult Scler* 2007; 13: 850–855.
14. de Luis DA, Varela C, de La Calle H, et al. *Helicobacter pylori* infection is markedly increased in patients with autoimmune atrophic thyroiditis. *J Clin Gastroenterol* 1998; 26: 259–263.
15. Emilia G, Longo G, Luppi M, et al. *Helicobacter pylori* eradication can induce platelet recovery in idiopathic thrombocytopenic purpura. *Blood* 2001; 97: 812–814.
16. Gasbarrini A, Franceschi F, Tartaglione R, et al. Regression of autoimmune thrombocytopenia after eradication of *Helicobacter pylori*. *Lancet* 1998; 352: 878.
17. Zentilin P, Savarino V, Garnero A, Accardo S, Seriolo B. Is *Helicobacter pylori* infection a risk factor for disease severity in rheumatoid arthritis? *Gastroenterology* 1999; 116: 503–504.
18. Montecucco C, de Bernard M. Molecular and cellular mechanisms of action of the vacuolating cytotoxin (Vac A) and neutrophil-activating protein (HP-NAP) virulence factors of *Helicobacter pylori*. *Microbes Infect* 2003; 5: 715–721.
19. Lucchinetti CF, Mandler RN, McGavern D, et al. A role for humoral mechanisms in the pathogenesis of Devic's neuromyelitis optica. *Brain* 2002; 125: 1450–1461.
20. Ishizu T, Osoegawa M, Mei FJ, et al. Intrathecal activation of the IL-17/IL-8 axis in opticospinal multiple sclerosis. *Brain* 2005; 128: 988–1002.
21. Minohara M, Matsuoka T, Li W, et al. Upregulation of myeloperoxidase in patients with opticospinal multiple sclerosis: positive correlation with disease severity. *J Neuroimmunol* 2006; 178: 156–160.
22. McDonald WI, Compston A, Edan G, et al. Recommended diagnostic criteria for multiple sclerosis: guidelines from the International Panel on the diagnosis of multiple sclerosis. *Ann Neurol* 2001; 50: 121–127.
23. Kira J, Kanai T, Nishimura Y, et al. Western versus Asian types of multiple sclerosis: immunogenetically and clinically distinct disorders. *Ann Neurol* 1996; 40: 569–574.
24. Matsushita T, Isobe N, Matsuoka T, et al. Aquaporin-4 autoimmune syndrome and anti-aquaporin-4 antibody-negative opticospinal multiple sclerosis in Japanese. *Mult Scler* 2009; 15: 834–847.
25. Wingerchuk DM, Hogancamp WF, O'Brien PC, Weinshenker BG. The clinical course of neuromyelitis optica (Devic's syndrome). *Neurology* 1999; 53: 1107–1114.

26. Kurtzke JF. Rating neurological impairment in multiple sclerosis: an expanded disability status scale (EDSS). *Neurology* 1983; 33: 1444–1452.
27. Ishizu T, Kira J, Osoegawa M, et al. Heterogeneity and continuum of multiple sclerosis phenotypes in Japanese according to the results of the fourth nationwide survey. *J Neurol Sci* 2009; 280: 22–28.
28. Fukazawa T, Hamada T, Tashiro K, Moriwaka F, Yanagihara T. Acute transverse myelopathy in multiple sclerosis. *J Neurol Sci* 1990; 100: 217–222.
29. Barkhof F, Filippi M, Miller DH, et al. Comparison of MRI criteria at first presentation to predict conversion to clinically definite multiple sclerosis. *Brain* 1997; 120: 2059–2069.
30. Kurtzke J, Page WF. Epidemiology of multiple sclerosis in US veterans: VII. Risk factors for MS. *Neurology* 1997; 48: 204–213.
31. Doi H, Matsushita T, Isobe N, et al. Hypercomplementemia at relapse in patients with anti-aquaporin-4 antibody. *Mult Scler* 2009; 15: 304–310.
32. Tanaka M, Matsushita T, Tateishi T, et al. Distinct CSF cytokine/chemokine profiles in atopic myelitis and other causes of myelitis. *Neurology* 2008; 71: 974–981.
33. Teneberg S, Miller-Podraza H, Lampert HC, et al. Carbohydrate binding specificity of the neutrophil-activating protein of *Helicobacter pylori*. *J Biol Chem* 1997; 272: 19067–19071.
34. Zanotti G, Papinutto E, Dundon W, et al. Structure of the neutrophil-activating protein from *Helicobacter pylori*. *J Mol Biol* 2002; 323: 125–130.
35. Algood HM, Gallo-Romero J, Wilson KT, Peek Jr RM, Cover TL. Host response to *Helicobacter pylori* infection before initiation of the adaptive immune response. *FEMS Immunol Med Microbiol* 2007; 51: 577–586.
36. Caruso R, Pallone F, Monteleone G. Emerging role of IL-23/IL-17 axis in *H pylori*-associated pathology. *World J Gastroenterol* 2007; 13: 5547–5551.
37. Calamita G. The *Escherichia coli* aquaporin-Z water channel. *Mol Microbiol* 2000; 37: 254–262.

Journal of the Neurological Sciences 288 (2010) 54–62

Contents lists available at ScienceDirect

Journal of the Neurological Sciences

journal homepage: www.elsevier.com/locate/jns

Induction of paranodal myelin detachment and sodium channel loss in vivo by *Campylobacter jejuni* DNA-binding protein from starved cells (C-Dps) in myelinated nerve fibers

Hua Piao [a,1], Motozumi Minohara [a,1], Nobutoshi Kawamura [a], Wei Li [a], Yoshimitsu Mizunoe [b], Fujio Umehara [c], Yoshinobu Goto [d], Susumu Kusunoki [e], Takuya Matsushita [a], Kazuhiro Ikenaka [f], Takashi Maejima [g], Jun-ichi Nabekura [g], Ryo Yamasaki [a], Jun-ichi Kira [a,*]

[a] Department of Neurology, Neurological Institute, Graduate School of Medical Sciences, Kyushu University, Fukuoka 812-8582, Japan
[b] Department of Bacteriology, Graduate School of Medical Sciences, Kyushu University, Fukuoka 812-8582, Japan
[c] Department of Neurology and Geriatrics, Kagoshima University Graduate School of Medical and Dental Sciences, Kagoshima University, 8-35-1 Sakuragaoka, Kagoshima 890-8520, Japan
[d] Department of Clinical Neurophysiology, Neurological Institute, Graduate School of Medical Sciences, Kyushu University, Fukuoka 812-8582, Japan
[e] Department of Neurology, Kinki University School of Medicine, 377-2 Ohno-Higashi, Osaka-Sayama, Osaka 589-8511, Japan
[f] Division of Neurobiology and Bioinformatics, National Institute for Physiological Sciences, 38 Myodaiji, Okazaki 444-8585, Aichi, Japan
[g] Division of Homeostatic Development, National Institute for Physiological Sciences, 38 Myodaiji, Okazaki 444-8585, Aichi, Japan

ARTICLE INFO

Article history:
Received 2 June 2009
Received in revised form 30 September 2009
Accepted 7 October 2009
Available online 31 October 2009

Keywords:
Guillain–Barré syndrome
Campylobacter jejuni
DNA-binding protein from starved cells
Axonal degeneration
Paranodal demyelination

ABSTRACT

In an axonal variant of Guillain–Barré syndrome (GBS) associated with *Campylobacter jejuni* (*C. jejuni*) enteritis, the mechanism underlying axonal damage is obscure. We purified and characterized a DNA-binding protein from starved cells derived from *C. jejuni* (C-Dps). This C-Dps protein has significant homology with *Helicobacter pylori* neutrophil-activating protein (HP-NAP), which is chemotactic for human neutrophils through binding to sulfatide. Because sulfatide is essential for paranodal junction formation and for the maintenance of ion channels on myelinated axons, we examined the *in vivo* effects of C-Dps. First, we found that C-Dps specifically binds to sulfatide by ELISA and immunostaining of thin-layer chromatograms loaded with various glycolipids. Double immunostaining of peripheral nerves exposed to C-Dps with anti-sulfatide antibody and anti-C-Dps antibody revealed co-localization of them. When C-Dps was injected into rat sciatic nerves, it densely bound to the outermost parts of the myelin sheath and nodes of Ranvier. Injection of C-Dps rapidly induced paranodal myelin detachment and axonal degeneration; this was not seen following injection of PBS or heat-denatured C-Dps. Electron microscopically, C-Dps-injected nerves showed vesiculation of the myelin sheath at the nodes of Ranvier. Nerve conduction studies disclosed a significant reduction in compound muscle action potential amplitudes in C-Dps-injected nerves compared with pre-injection values, but not in PBS-, heat-denatured C-Dps-, or BSA-injected nerves. However, C-Dps did not directly affect Na^+ currents in dissociated hippocampal neurons. Finally, when C-Dps was intrathecally infused into rats, it was deposited in a scattered pattern in the cauda equina, especially in the outer part of the myelin sheath and the nodal region. In C-Dps-infused rats, but not in BSA-infused ones, a decrease in the number of sodium channels, vesiculation of the myelin sheath, axonal degeneration and infiltration of Iba-1-positive macrophages were observed. Thus, we consider that C-Dps damages myelinated nerve fibers, possibly through interference with paranodal sulfatide function, and may contribute to the axonal pathology seen in *C. jejuni*-related GBS.

1. Introduction

An axonal variant of Guillain–Barré syndrome (GBS) is associated with *Campylobacter jejuni* (*C. jejuni*) enteritis [1]; however, the mechanism underlying axonal damage is obscure. It was reported that, in this condition, the earliest changes are nodal lengthening and paranodal demyelination [2]. Although anti-GM1 ganglioside antibody is assumed to be pathogenic [3], reproduction of either the clinical or pathological components of the disease by passive transfer of anti-GM1 antibodies to experimental animals has never been successful [4–6]. Thus, the role of anti-GM1 antibodies in axonal GBS remains to be elucidated, and further studies on other factors are required.

We purified and characterized a DNA-binding protein from starved cells (Dps) derived from *C. jejuni* [7]. The C-Dps protein was found to share 41% and 24% amino acid identities with *Helicobacter pylori* neutrophil-activating protein (HP-NAP) and *Escherichia coli* (*E. coli*) Dps, respectively. These proteins constitute the Dps protein family, are produced at high levels under conditions of oxidative or nutritional stress, and efficiently

* Corresponding author. Tel.: +81 92 642 5340; fax: +81 92 642 5352.
E-mail address: kira@neuro.med.kyushu-u.ac.jp (J. Kira).
[1] These authors contributed equally to this work.

0022-510X/$ – see front matter © 2009 Elsevier B.V. All rights reserved.
doi:10.1016/j.jns.2009.10.007

protect bacterial DNA from damages. HP-NAP lacks DNA-binding capability, but through binding to neutrophil glycosphingolipids, such as sulfatide, it is chemotactic for human neutrophils [8]. Recently, sulfatide was found to be essential for paranodal junction formation and for the maintenance of ion channels on myelinated axons [9,10]. In addition, anti-sulfatide antibody is frequently found in dysimmune neuropathy patients presenting with demyelination and prominent axonal involvement [11,12], and passive transfer of the antibody induces similar pathology [13]. These findings prompted us to clarify the effects of C-Dps on myelinated axons and the possible involvement of C-Dps in *C. jejuni*-related GBS. For this purpose, we first studied specific binding of C-Dps to sulfatide by ELISA, immunostaining of thin-layer chromatograms loaded with various glycolipids, and double immunostaining of the peripheral nerves by anti-C-Dps and anti-sulfatide antibody, and then applied C-Dps onto peripheral nerves by intraneural injection and intrathecal infusion. Moreover, we also investigated the direct actions of C-Dps on sodium channels using dissociated hippocampal neurons expressing sodium channels. Here, we report the induction of paranodal myelin detachment and axonal degeneration by C-Dps in myelinated fibers.

2. Materials and methods

2.1. Purification of recombinant C-Dps protein

E. coli BL21 (DE3) cells harboring the *dps* gene were grown in LB-ampicillin (50 μg/ml) at 37 °C overnight. After expression of *dps* was induced with 1 mM isopropyl-D-thiogalactoside for 3 h, bacterial cells were harvested (15,000×*g* for 1 h) and resuspended in 20 mM Tris–HCL buffer (pH 8.0). After cell disruption by sonication, the lysates were centrifuged at 4 °C (39,000×*g* for 20 min). Supernatants containing C-Dps were purified using Ni–NTA agarose columns and dialyzed against PBS—0.1 mM EDTA [7]. Thereafter, endotoxin levels were decreased by affinity chromatography using a polymyxin B agarose gel (Sigma, MO, USA). We assayed the endotoxin level in the final protein solution using a QCL-1000 kit (BioWhittaker, Belgium), and the levels were found to be less than 10 EU/mg.

2.2. Generation of a monoclonal antibody to C-Dps

For the generation of a monoclonal antibody against C-Dps, BALB/c mice were immunized with a recombinant C-Dps protein [7]. After four injections at 3 week intervals, spleen cells obtained from immunized BALB/c mice were fused with mouse P3U1 myeloma cells. Hybridoma supernatants were screened by ELISA. Subcloning of positive hybridomas was done using standard techniques. Immunoglobulin G (IgG) was purified by protein G column chromatography.

2.3. ELISA for C-Dps binding to gangliosides

We coated polystyrene microtiter ELISA plates (ICN Biomedicals, Inc., USA) with 200 ng of bovine brain ganglioside type III, GM1, GM2, GM3, GD1a, GD1b, GD3, GT1b, galactocerebroside, sulfatide (Sigma), and GQ1b (Calbiochem, CA, USA), and dried them by evaporation. After incubation with 1% bovine serum albumin (BSA) in PBS for 30 min, 50 μl of C-Dps protein (0.5 μg/ml) was added to each well at room temperature for 1 h. Uncoated wells treated with C-Dps were used as controls. For quantitative measurements, we applied 50 μl of C-Dps protein (0, 0.125, 0.25, 0.5, 1, 2, or 4 μg/ml) to the plates coated with GM2, GD1a, and sulfatide (200 ng of each). After washing wells with PBS, 50 μl of anti-C-Dps IgG mAb (1:5000) was added to each well at room temperature and incubated for 1 h. After further washing, 50 μl of HRP-conjugated anti-mouse IgG (1:2000) (Vector Laboratories, CA, USA) was added and incubated at room temperature for 1 h. After washing, a color reaction was obtained by adding *o*-phenylenediamine dihydrochloride (Sigma; 100 μl/well), and incubating at room temperature for 15 min. The reaction was stopped by the addition of 50 μl of 4 N H_2SO_4, and the optical density (OD) was measured at 450 nm.

2.4. Thin-layer chromatogram immunostaining

Glycolipids were separated on Polygram Sil G thin-layer chromatogram (TLC) plates (Macherey-Nagel Gmbh & Co., Germany). The plates were developed in chloroform–methanol–0.2% $CaCl_2$ (50:45:10, v/v/v) and glycolipids were detected by orcinol spray. After separating the lipids, the TLC plates were dipped in *n*-hexane containing 0.4% poly (isobutyl)methacrylate for 1 min and air-dried. After incubation in 1% BSA in PBS for 30 min, each plate was incubated for 1 h with or without C-Dps protein (1 μg/ml) at room temperature. After washing, the plates were incubated with a mouse anti-C-Dps mAb (1:5000) for 1 h at room temperature and developed with an HRP-conjugated anti-mouse-IgG antibody (1:200) for 1 h at room temperature. After the last wash, a color reaction was developed using 0.5 mg/ml 3,3′-diaminobenzidine tetrahydrochloride (Sigma) in PBS containing 0.01% H_2O_2.

2.5. C-Dps binding to the peripheral nerve tissue

To study C-Dps binding to peripheral nervous tissues, 8-week-old female Lewis rats were fixed by transcardial perfusion with 2% paraformaldehyde in PBS. Sciatic nerves were harvested and incubated in collagenase type IV in PBS for 20 min at room temperature. After washing, the nerves were de-sheathed and teased into small bundles of fibers under a stereomicroscope. The teased fibers were incubated in blocking buffer (5% goat serum and 1% BSA in PBS) for 15 min. After blocking, they were incubated with C-Dps (5 μg/ml) at room temperature for 1 h. Control fibers were incubated without C-Dps. For double immunostaining, anti-C-Dps mAb (1:5000) and mouse anti-O4 IgM antibody recognizing sulfatide (1:200) (R&D Systems, Minneapolis, MN, US) were applied to fibers and incubated at room temperature for 1 h followed by incubation with Alexa Fluor 488 anti-mouse IgG (1:1000) or Alexa Fluor 594 anti-mouse IgM (1:1000) (Molecular Probes, OR, USA). Images were captured by confocal laser scanning microscopy (CLSM, Fluoview FV300, Olympus, Japan).

2.6. Intraneural injection of C-Dps

To examine the effects of C-Dps *in vivo*, the effect of an intraneural injection of C-Dps was investigated. Eight-week-old Lewis rats (female) were anesthetized by intraperitoneal injections of 40–50 mg/kg sodium pentobarbital. The sciatic nerve was exposed by an aseptic surgical incision from the sciatic notch to the popliteal fossa and 15 μg (30 μl) of C-Dps was injected intraneurally at the mid-thigh level. As controls, PBS alone, 15 μg (30 μl) of heat-denatured C-Dps (100 °C, 30 min) or 15 μg (30 μl) of BSA was injected into the contralateral side. All injections were done using a hand-held microsyringe fitted with a 30 1/2-gauge needle under a dissecting microscope. Four hours after the intraneural injection, rats were kept anesthetized and the tissues were fixed by transcardial perfusion with 4% paraformaldehyde. Animals were sacrificed and the sciatic nerves were harvested. All rats were kept normothermic at 36.5–37.5 °C using a heat lamp. All experiments conformed to the Guiding Principles for the Care and Use of Animals approved by the Council of Kyushu University.

2.7. Neuropathological studies

The harvested sciatic nerves and cauda equina were coated with OCT (Sakura Finetek, CA, USA) and cut into 10-μm sections in the longitudinal and transverse planes. Immunohistochemistry with an anti-C-Dps mAb was used to detect if C-Dps had bound to neural tissues. The sections were incubated in blocking buffer (5% goat serum and 1% BSA in PBS) for 15 min. After blocking, they were incubated

with anti-C-Dps mAb (1:5000) or an anti-neurofilament (NF) polyclonal antibody (1:200) (Chemicon, MA, USA) in blocking buffer for 1 h at room temperature. Binding of these antibodies was detected by incubating sections with Alexa Fluor 488 anti-mouse IgG (1:1000) or Alexa Fluor 594 anti-rabbit IgG (1:1000) (Molecular Probes). Sections from rats that had undergone intrathecal infusion were incubated with blocking buffer for 15 min and then incubated for 1 h at room temperature with anti-ionized calcium-binding adapter molecule-1 (Iba-1) antibody (1:2000) (Wako, Japan). Biotinylated goat anti-rabbit antibody (undiluted solution) and peroxidase-conjugated streptavidin (undiluted solution) (Nichirei, Japan) were used as secondary antibodies. The colored reaction product was developed using Simple Stain DAB solution (Nichirei). The sections were counterstained lightly with hematoxylin. The frequency of affected nerves was evaluated in an examiner-blinded fashion based on the presence or absence of abnormal fiber changes (vesiculation of myelin or axonal degeneration on cross-sections). For comparison of the frequencies of affected nerves, more than 100 nerve fibers were counted in each animal and six to ten rats were included in each experimental group.

2.8. Immunohistochemistry in teased sciatic nerve fibers

Teased sciatic nerve fibers from intraneurally injected Lewis rats were prepared and incubated in blocking buffer for 15 min. After blocking, they were incubated with biotin-conjugated peanut agglutinin (PNA) (10 μg/ml) (Vector Laboratories), anti-sodium channel Scn8a antibody (1 μg/ml) (Sigma), anti-contactin-associated protein (Caspr) antibody (1:1000) (a marker for paranodal junctions between the axonal membrane and terminal loop of myelinated glial cells; a kind gift from Dr. E. Peles, Weizmann Institute, Israel), anti-myelin basic protein antibody (1:200) (Acris Antibodies GmbH, Germany) or an anti-NF antibody (1:400) in blocking buffer for 1 h at room temperature. Binding of these antibodies was detected by incubating fibers with dichlorotriazinyl amino fluorescein (DTAF)-conjugated streptavidin (Immunotech, France), Alexa Fluor 488 anti-mouse IgG (1:1000) or Alexa Fluor 594 anti-rabbit IgG (1:1000). Images were captured by CLSM.

2.9. Teased fiber analysis and electron microscopy for C-Dps-injected sciatic nerves

A portion of each sciatic nerve specimen was fixed overnight in 3% glutaraldehyde in 0.125 M cacodylate buffer (pH 7.4), washed, osmicated and embedded in epon. A 2–3-mm portion proximal to the injection site was embedded in epon to obtain a cross-section. The portion of the specimen distal to the cross-section (about 5 mm in length) was fixed in the same glutaraldehyde solution, washed and osmicated for teased-fiber analysis. Semi-thin sections were made for light microscopy and ultra-thin sections were made for electron microscopy. In the teased fiber analysis, the percentages of abnormal fibers were evaluated by counting the number of abnormal fibers (showing paranodal demyelination or axonal degeneration) among one hundred nerve fibers in each animal; six rats were included in each experimental group.

2.10. Nerve conduction study

Stainless steel needle electrodes were used for stimulation and recording. One pair of stimulating electrodes was positioned on the sciatic nerve at the mid-thigh level and compound muscle action potentials (CMAPs) were recorded using two pairs of recording electrodes penetrating the intrinsic foot muscles. Ground electrodes were placed either side of the recording electrodes. CMAPs were amplified by a Dual Bio Amp ML 135 amplifier (Cygnus Technology, PA, USA) and analyzed using Scope software (v3.7.1; AD Instruments Powerlab 2/20, NSW, Australia). Recordings were obtained immediately before injection and at 10, 60, 180, 300 and 420 min after injection. Peak to peak amplitudes and latencies of the first peaks were measured. To assess the presence of a conduction block, one of the electrophysiological correlates of acute demyelination, the proximal to distal (P/D) amplitude ratio of CMAPs, was calculated [14]. This method minimizes changes in the absolute amplitudes resulting from variations in electrode placement during different recording sessions in the same animal.

2.11. Patch-clamp recording of Na^+ currents using dissociated hippocampal CA1 neurons

Mechanically isolated hippocampal neurons prepared from Wistar rats (postnatal days 12–14) were whole-cell clamped at room temperature in an external solution containing (in mM) 140 NaCl, 2.5 KCl, 10 HEPES, 2 $CaCl_2$, 1 $MgCl_2$, and 10 glucose (pH 7.4, adjusted with Tris–OH), as described previously [15]. The pipette solution contained (in mM) 5 KCl, 130 K–D–gluconate, 10 NaCl, 10 HEPES, 0.5 EGTA, 4 Mg–ATP and 0.4 Na–GTP (pH 7.3, adjusted with KOH). Pipette resistance was 3–5 MΩ. Currents were acquired using an Axopatch 200B amplifier, filtered at 5 kHz (internal low-pass Bessel filter) and sampled at 40 kHz using pClamp8 software through a Digidata 1322A interface. Neurons were held at −60 mV. Capacity transients were cancelled and series resistance was compensated by 70–80%. Using a "Y-tube system", the external solution was focally applied to neurons and rapidly exchanged for a solution containing C-Dps (5 μg/ml). One-hundred-millisecond voltage pulses to −20 mV preceded by 100-ms pre-pulses to −100 mV evoked transient large inward currents followed by steady outward currents.

2.12. Intrathecal infusion of C-Dps

Intrathecal infusion of C-Dps (0.06 mg/kg/day for 10 days, $n=6$) or BSA (0.06 mg/kg/day for 10 days, $n=6$) was performed. Eight-week-old Lewis rats (female) were anesthetized and a T10 laminectomy was carried out to expose the underlying thoracic spinal cord segments. After the dura was carefully punctured, a polyethylene tube (PE-10) (Becton Dickinson, NJ, USA) was inserted into the subarachnoid space. The PE-10 tube was connected to an osmotic pump (Alzet 2002) (Alzet Corp., CA, USA) through a PE-60 tube, which was then inserted into the subcutaneous space via a sterile surgical procedure. *Salmonella typhimurium* lipopolysaccharide (LPS) (Sigma) (3 mg/kg in 200 μl PBS) was given intraperitoneally on days 4 and 7. Disruption of the blood nerve barrier (BNB) was confirmed by injection of Evans blue-labeled BSA (67 kDa) (Sigma) 23 h after intraperitoneal injection of LPS in preliminary experiments. On day 10, animals were sacrificed, and the sciatic nerves and cauda equina were harvested.

2.13. Statistical analysis

We used two-way repeated-measures ANOVAs and Bonferroni post-tests to compare the OD values from ELISA experiments. The frequencies of affected nerves were compared using Fisher's exact probability test. In the teased fiber analysis, abnormal fiber percentages were analyzed using the Mann–Whitney U test. Results of nerve conduction studies are expressed as means ± S.D. Mean P/D amplitude ratios and the motor conduction velocity (MCV) of sciatic nerves after injection with C-Dps, PBS and heat-denatured C-Dps were compared with the pre-injection values using a Wilcoxon signed-rank test. Statistical significance was set at $P<0.05$. Data from patch-clamp recordings are expressed as means ± SEM and statistical analysis was performed using a Student's t test.

3. Results

3.1. C-Dps binding to sulfatide

We searched for the molecular target of C-Dps among glycolipids by analogy to HP-NAP [13]. Analysis by ELISA, using microtiter wells coated with various glycolipids, revealed that C-Dps adsorbed to sulfatide alone, but not to GM1, GM2, GM3, GD1a, GD1b, GD3, GT1b, GQ1b or galactocerebrosides (Fig. 1A). C-Dps dose-dependently bound to sulfatide, but not to GM2 or GD1a (Fig. 1B). Furthermore, immunostaining of TLCs loaded with the above-mentioned glycolipids confirmed that C-Dps strongly bound to sulfatide only (Fig. 1C), in a manner analogous to that of HP-NAP [13]. Double immunostaining with anti-C-Dps antibody and anti-O4 antibody on teased nerve fibers exposed to C-Dps revealed co-localized immunostaining of C-Dps and sulfatide (Fig. 1D).

3.2. Morphological effects of C-Dps injected into the rat sciatic nerve

In teased nerve fiber specimens of PBS-injected sciatic nerves, double immunostaining for sodium channels and Caspr, and for Caspr and NF, showed clustering of sodium channels at the nodes of Ranvier, which were scattered along the nerve fibers (Fig. 2A). On the other hand, in C-Dps-injected sciatic nerves, C-Dps was found to be deposited at the nodes of Ranvier and on the outer surface of internodal myelin. Furthermore, decreased and patchy immunoreactivity for sodium channels was observed in the nodes of Ranvier (Fig. 2B). Immunoreactivity for Caspr, a marker of paranodes, was also impaired in C-Dps-injected nerves (Fig. 2B). In epon-embedded sections, C-Dps-injected nerves showed various changes, such as vesiculation of the myelin sheath, intramyelinic edema and axonal degeneration, compared with the control groups (PBS-injected and heat-denatured C-Dps-injected sciatic nerves) (Fig. 3A). The frequency of affected nerves showing either vesiculation of the myelin sheath or axonal degeneration on cross-sections was significantly higher in the C-Dps-injected group than in the control group (83.3% vs. 20.0%, $P=0.0350$) (Fig. 3C). In teased fiber analysis, C-Dps-injected sciatic nerves showed paranodal demyelination and axonal degeneration more frequently than the control group (Fig. 3B). The abnormal fiber percentage in C-Dps-injected nerves was significantly greater than that in control nerves (6.0% vs. 0.7%, $P=0.0457$) (Fig. 3C). Electron microscopically, C-Dps-injected nerves showed disruption of the myelin terminal loop and vesiculation of the myelin sheath at the nodes of Ranvier (Fig. 4).

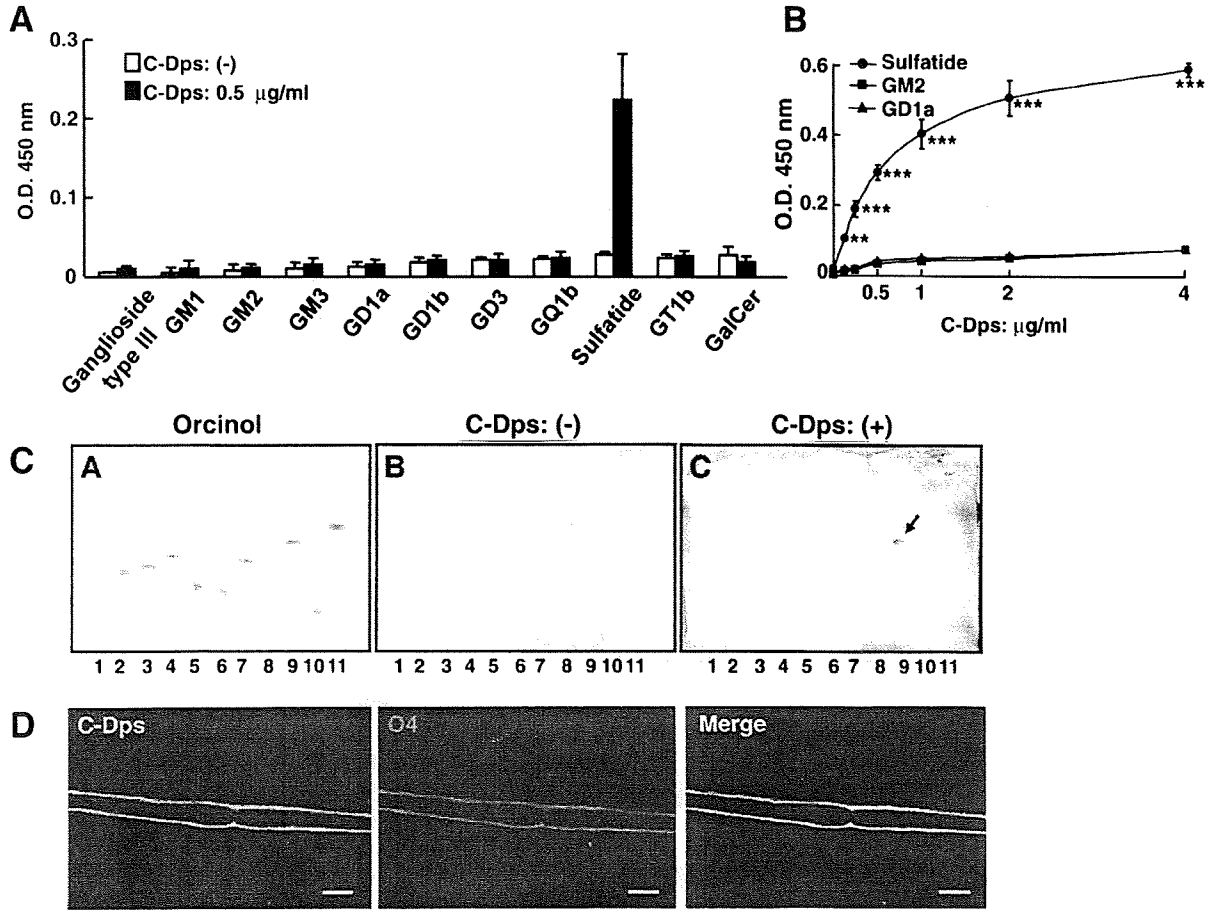

Fig. 1. C-Dps specifically binds to sulfatide. A. An ELISA assay using microtiter plates coated with bovine brain ganglioside type III, GM1, GM2, GM3, GD1a, GD1b, GD3, GT1b, GQ1b, galactocerebroside and sulfatide shows C-Dps binding to sulfatide only. The experiments were repeated four times and the bars indicate the standard errors. B. An ELISA assay shows dose-dependent C-Dps binding to sulfatide, but not to GM2 or GD1a (**$P<0.01$, ***$P<0.001$). The experiments were repeated three times and the bars indicate the standard deviations. C. Immunostaining of thin-layer chromatograms loaded with the above-mentioned glycolipids demonstrates strong staining for sulfatide (arrow) only. Panel A shows orcinol staining, while panels B and C show plates overlaid with PBS and C-Dps, respectively, immunostained with anti-C-Dps mAb and a peroxidase-conjugated anti-mouse IgG antibody. In panels A–C, lanes show bovine brain ganglioside type III (lane 1), GM1 (lane 2), GM2 (lane 3), GM3 (lane 4), GD1a (lane 5), GD1b (lane 6), GD3 (lane 7), GQ1b (lane 8), sulfatide (lane 9), GT1b (lane 10) and galactocerebroside (lane 11). C-Dps = *Campylobacter jejuni* DNA-binding protein from starved cells, O.D. = optical density. D. Double immunostaining with anti-C-Dps antibody and anti-O4 (sulfatide) antibody on teased sciatic nerve fibers exposed to C-Dps shows C-Dps binding to the outer part of the myelin sheath, where the co-localization with sulfatide is seen. Scale bars = 10 μm.